MUSE Simulation

Steffen Strauch
University of South Carolina

for the MUSE Collaboration

Supported in parts by the U.S. National Science Foundation: NSF PHY-2111050 (USC).
The MUSE experiment is supported by the U.S. Department of Energy, the U.S. National Science Foundation, the Paul Scherrer Institute, and the US-Israel Binational Science Foundation.

MUSE Review, BVR 54, PSI, January 23, 2023

Recent updates of the MUSE simulation

- More detailed and accurate geometry
- Flexible alignment of components
- More realistic particle beam
- Digitization of simulated events
- Realistic event generator to study radiative effects, ep→ epγ [BVR 52]

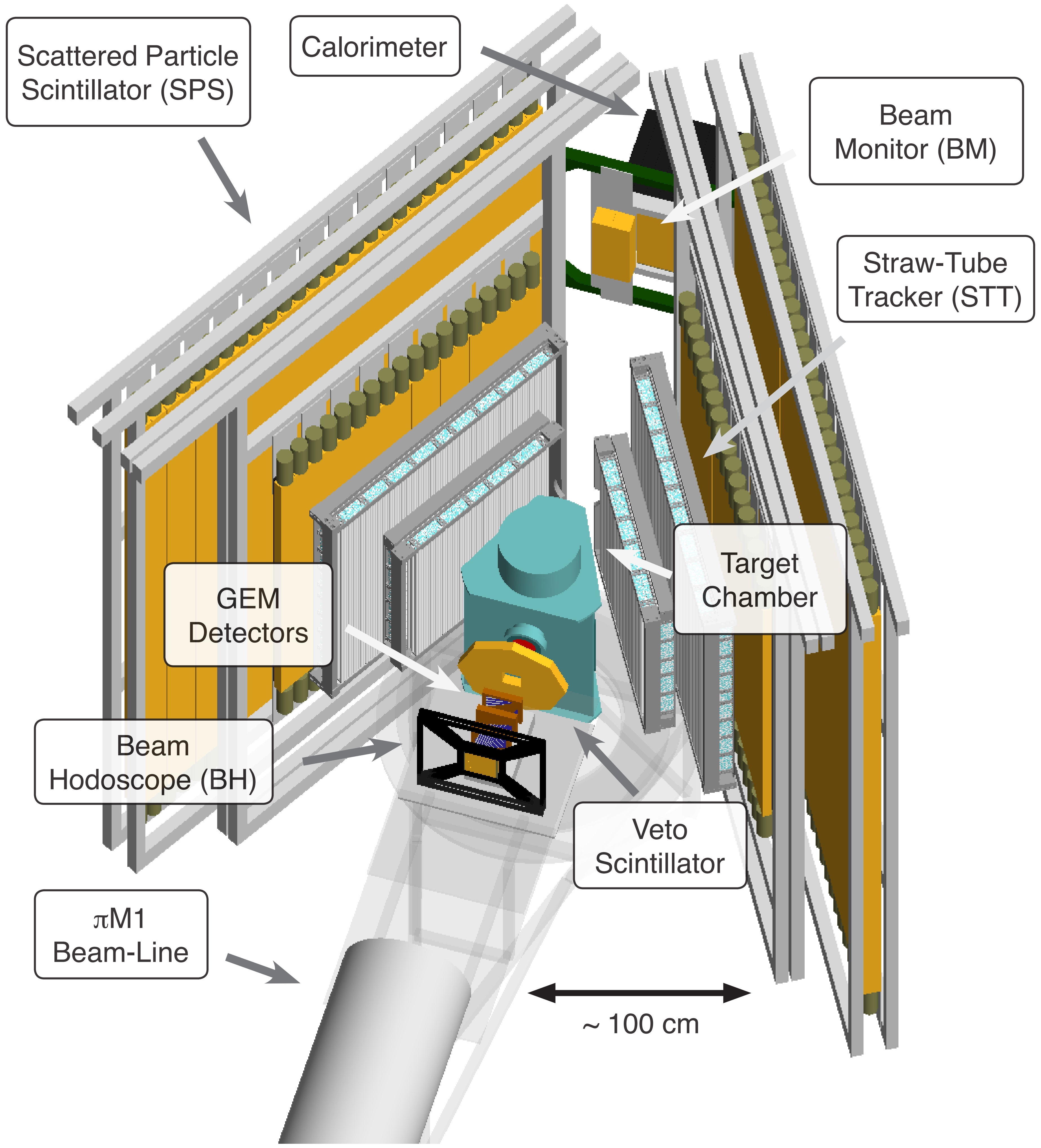

Implementation of the STT frames in the MUSE simulation

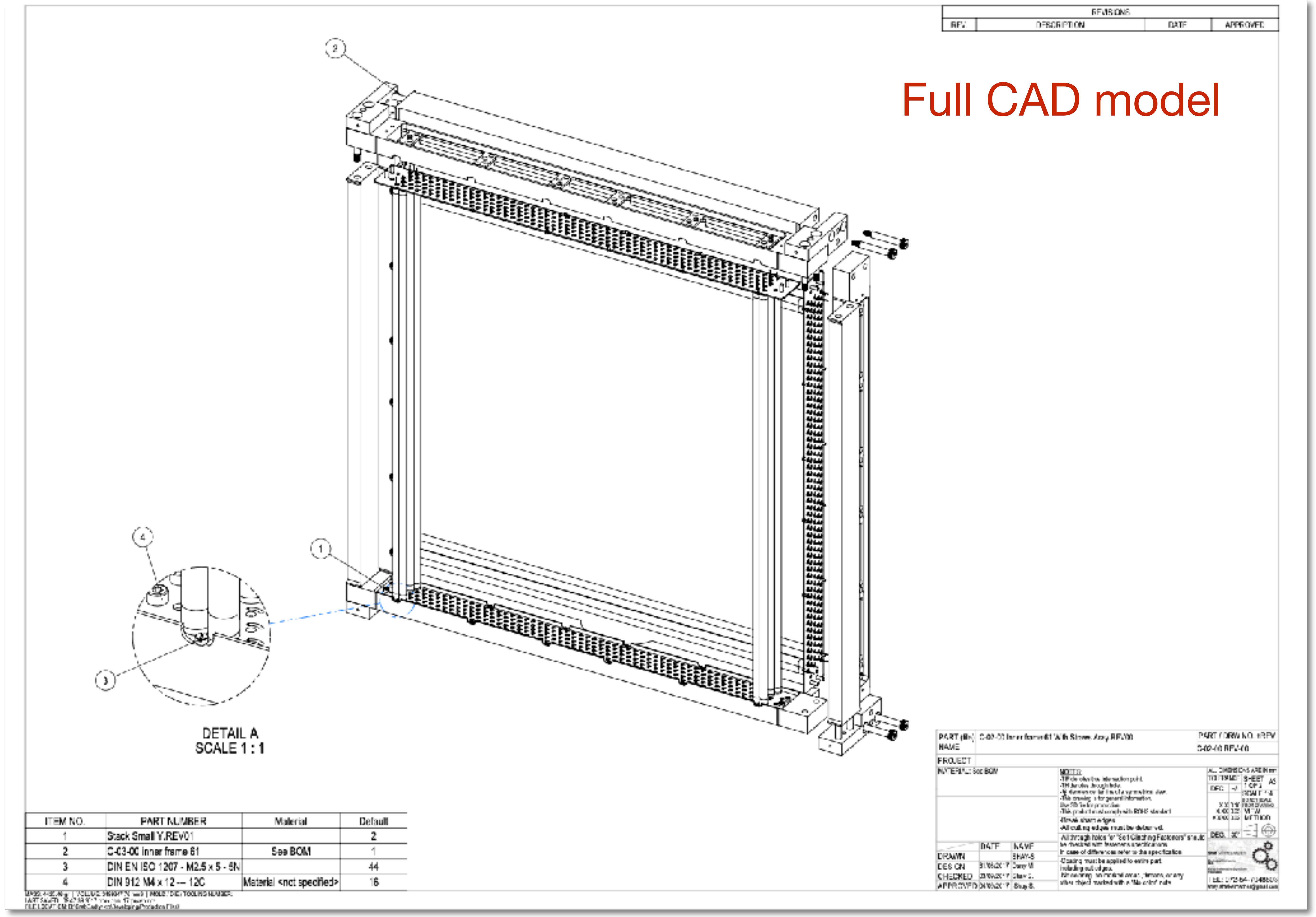

Simplified CAD model (Tom O'Connor, ANL) with detail in outer surface maintained

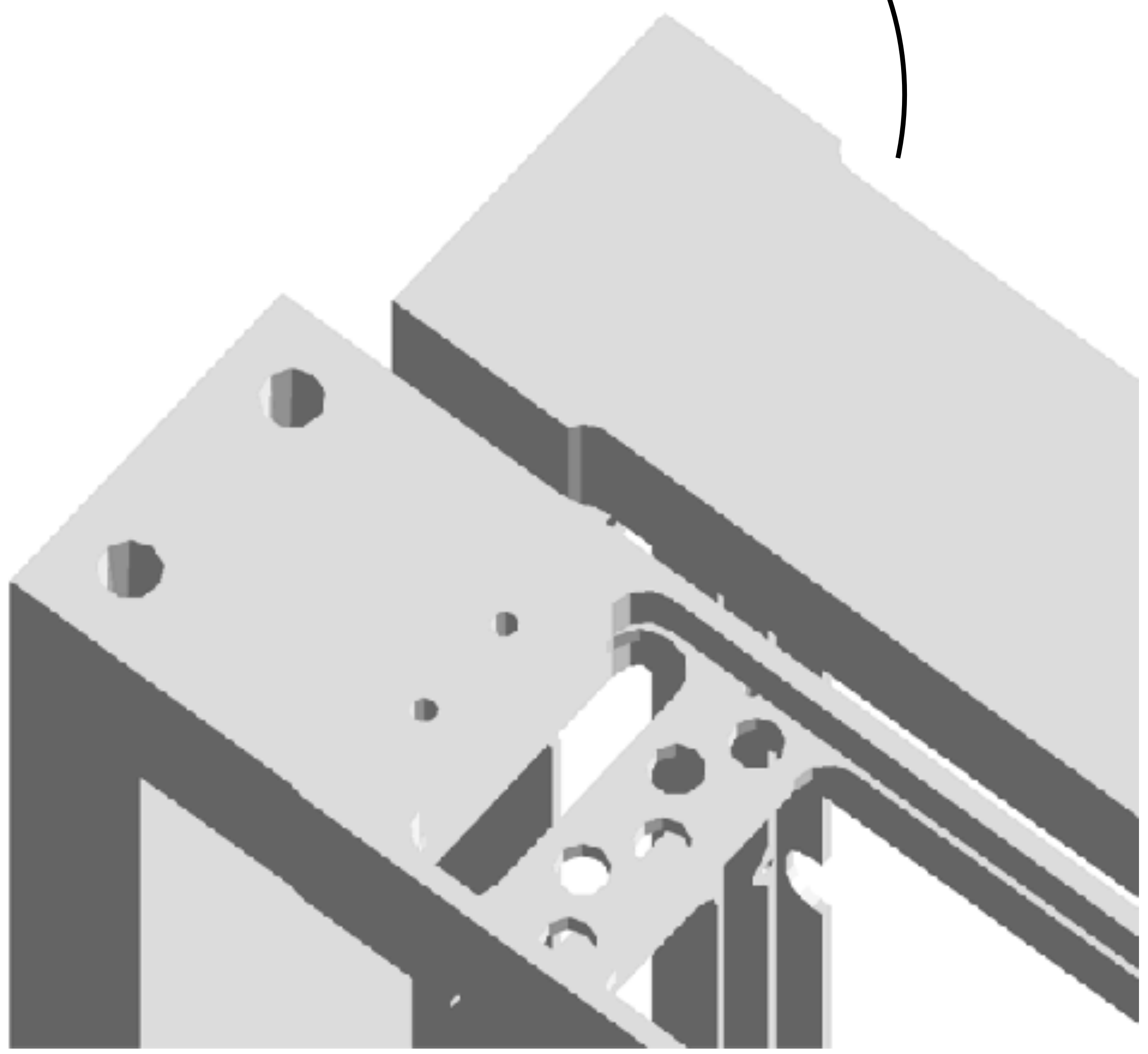

Binary STL files can now be loaded directly in the simulation.

More work needed to bring all relevant structure material into the simulation.

Reimplementation of target ladder including carbon target

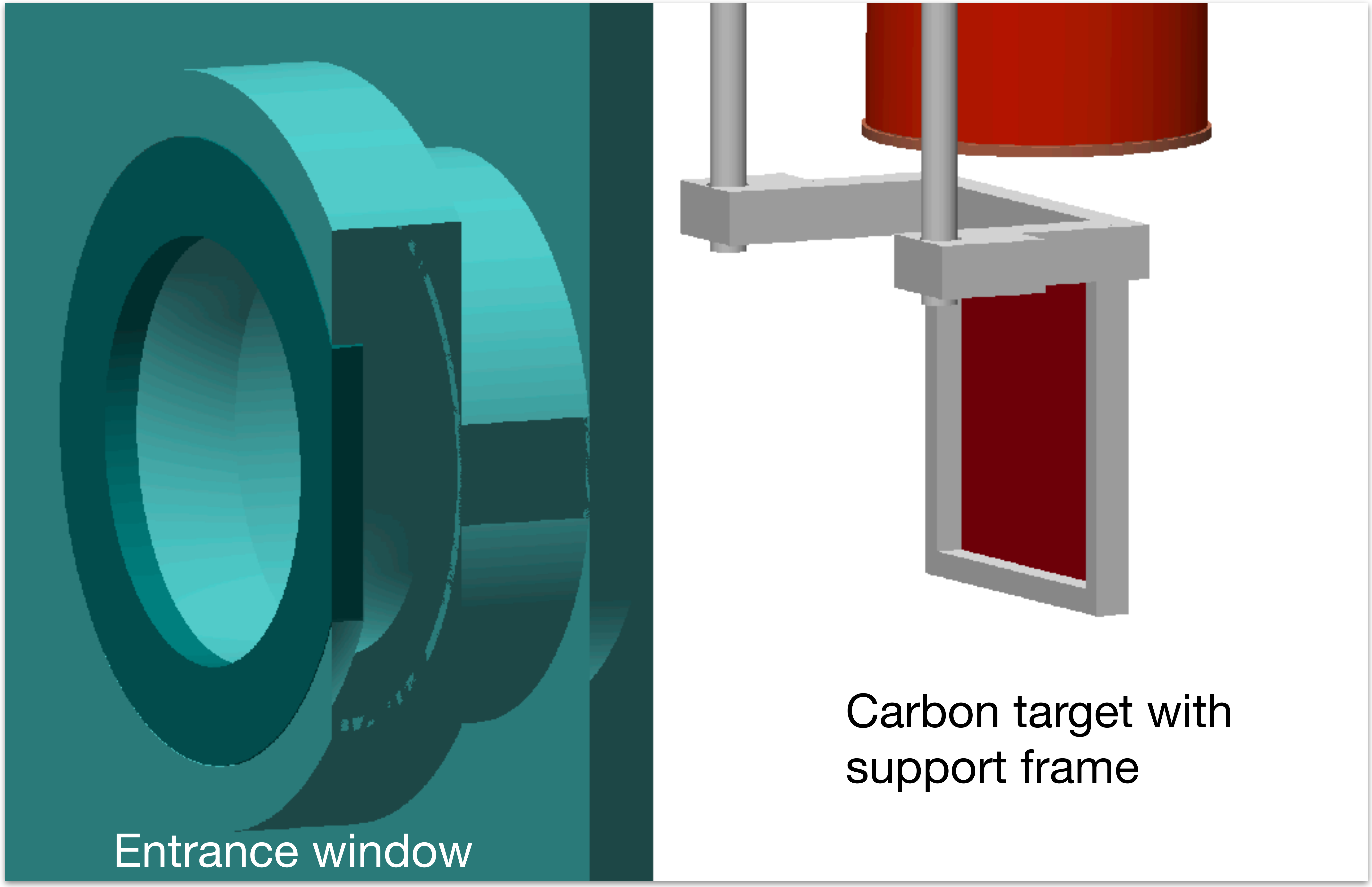

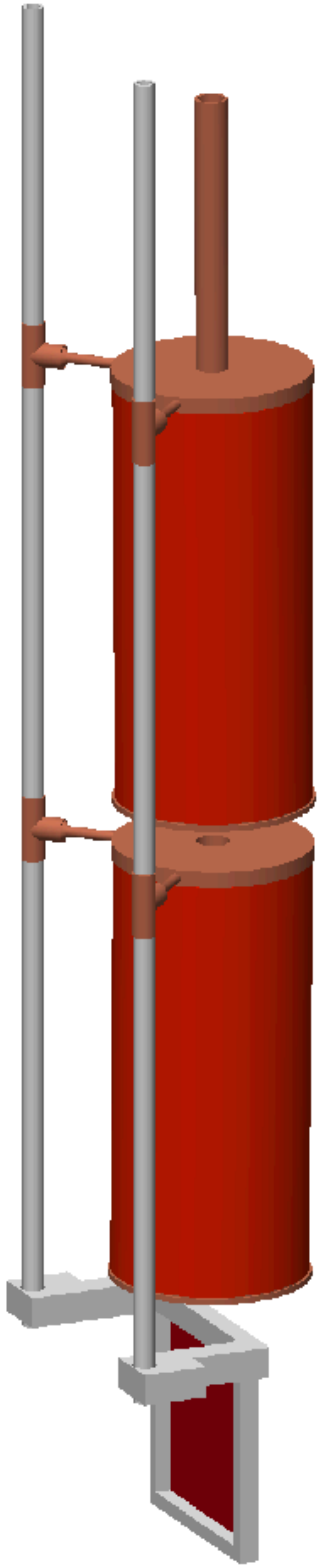

Target ladder with LH2, dummy, and carbon targets

Not included yet: beam-focus monitor

Implementation: Stefan Lunkenheimer

Scattering off the target chamber contributes significantly to the total DAQ rate

Simulated scattering-chamber hits by a 161 MeV/c electron beam with trigger on the beam-left (x > 0) SPS detectors, no target

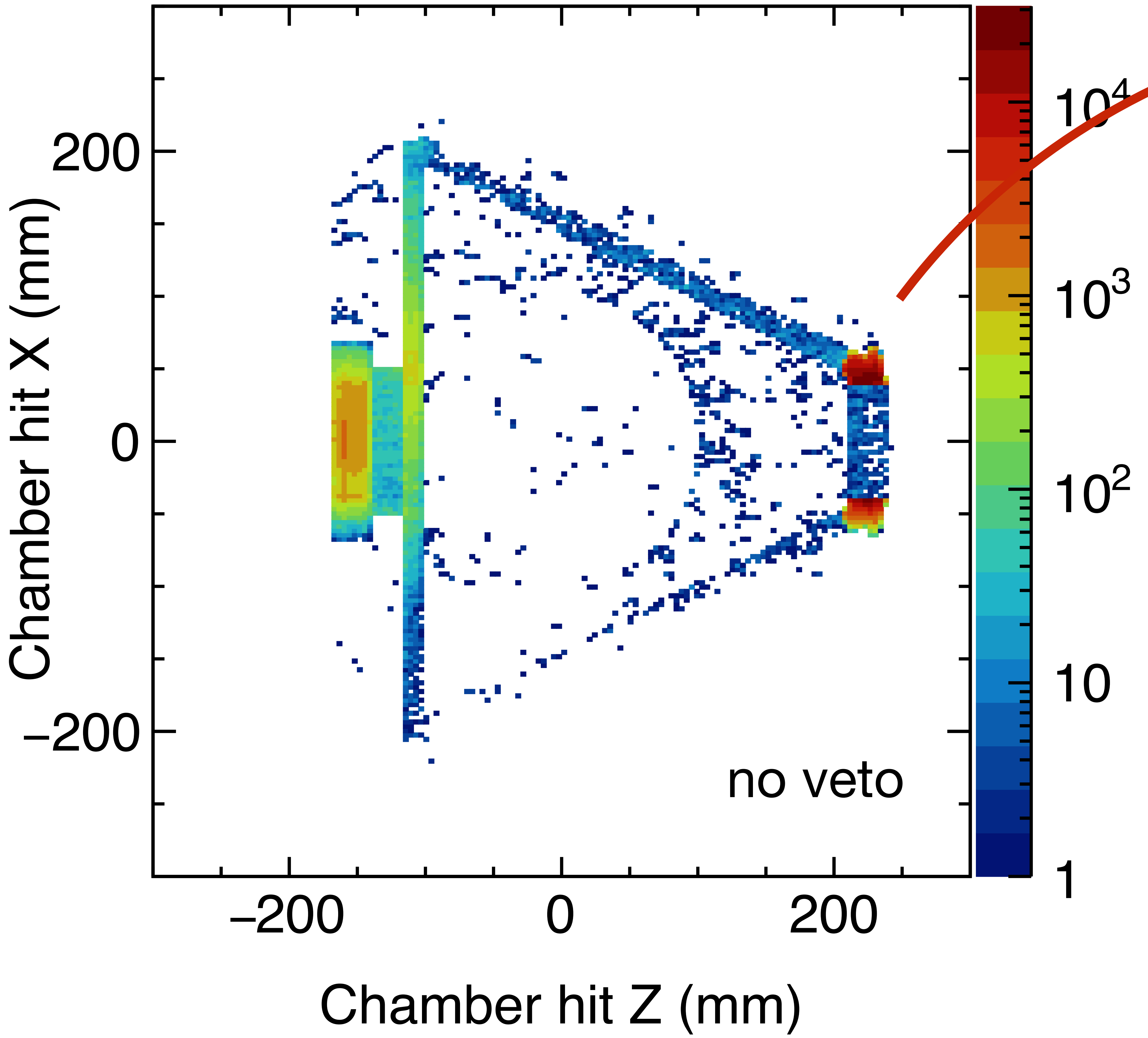

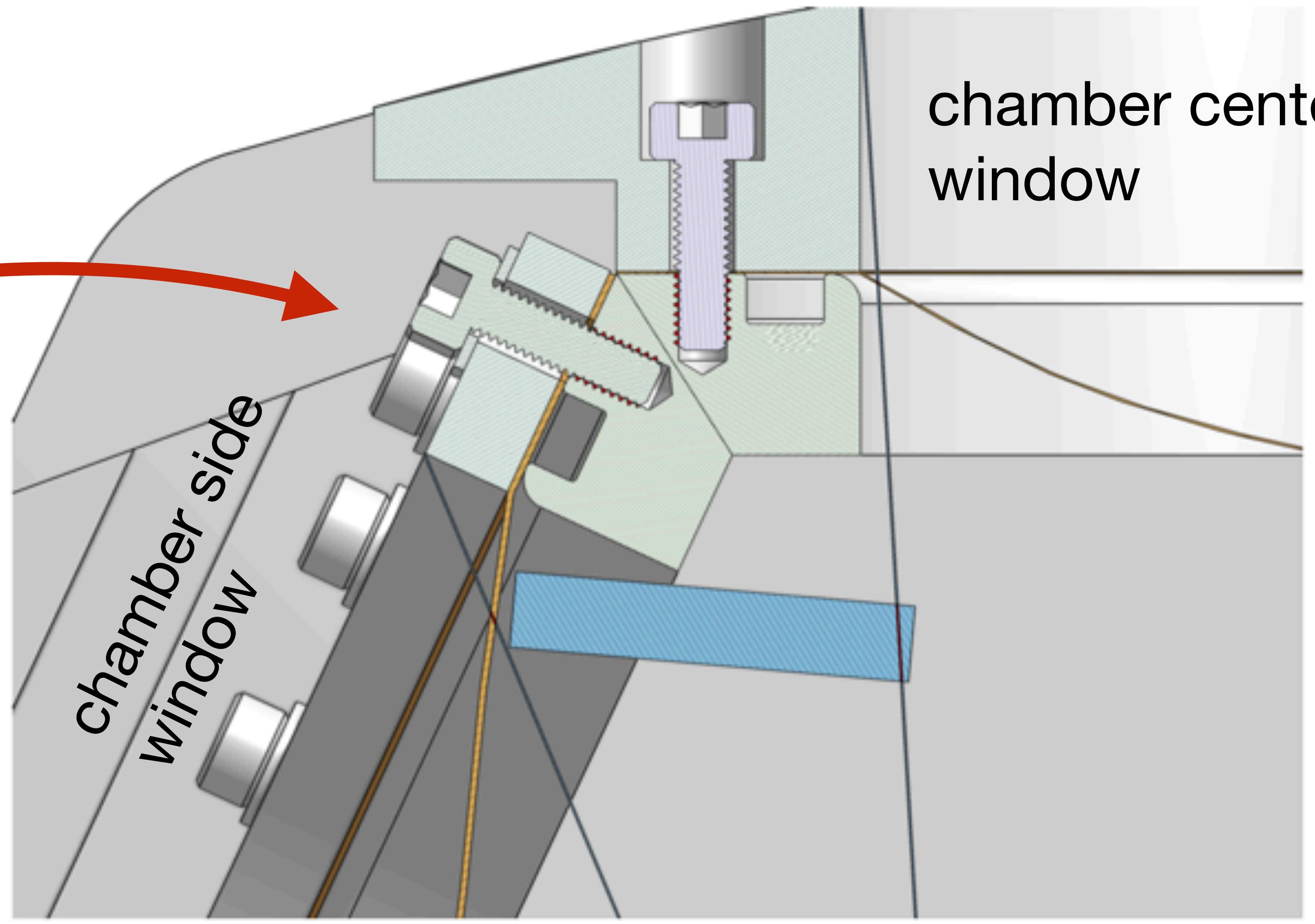

Target chamber post veto detector:

(T. Rostomyan)

- Must be inside of the chamber.
- Maximum coverage of chamber posts, while
- clearing the acceptance of scattering and straight through events, and
- clearing in-bound chamber side window

Anticipated suppression of chamber hits: Fewer than 10% remaining

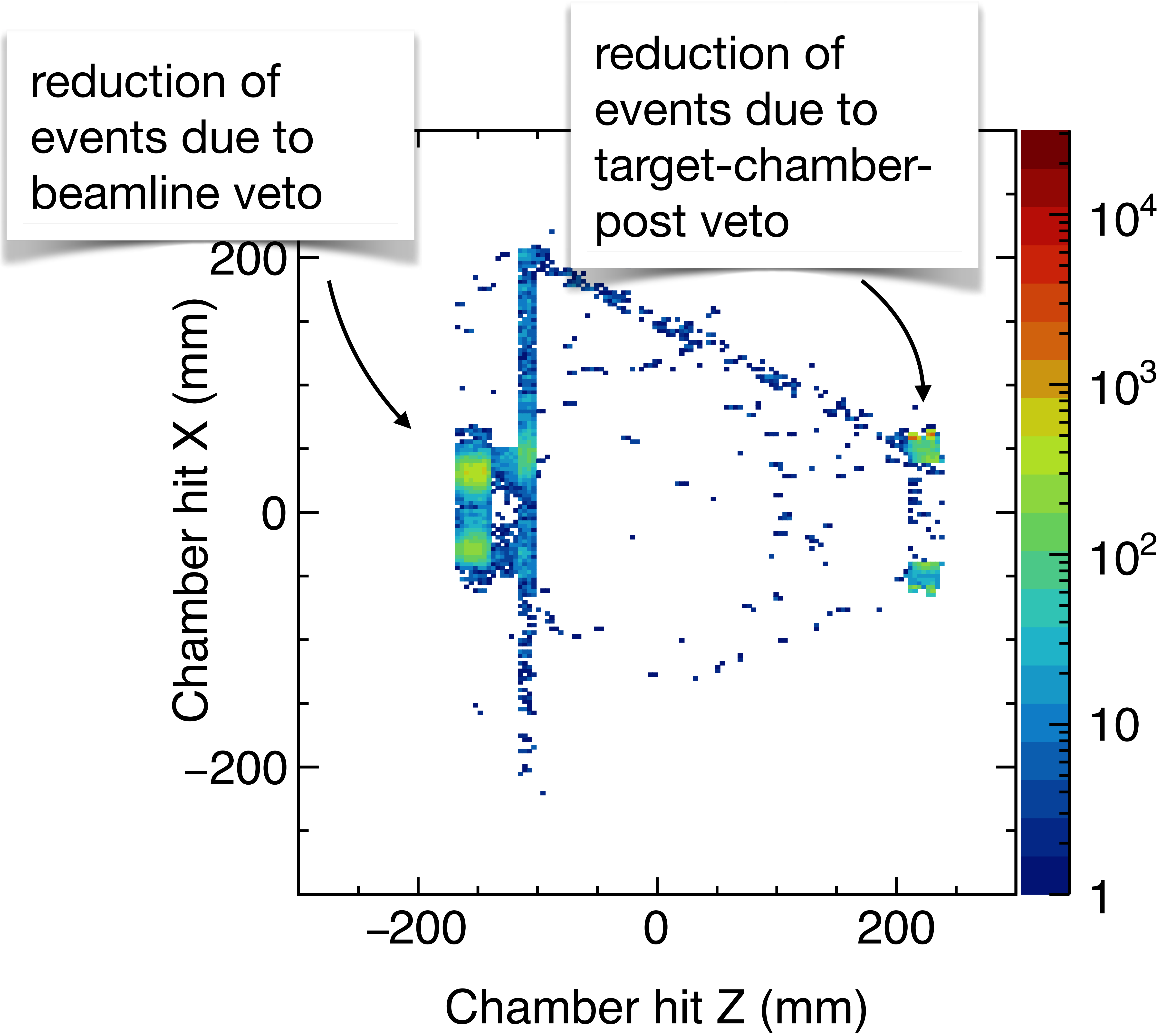

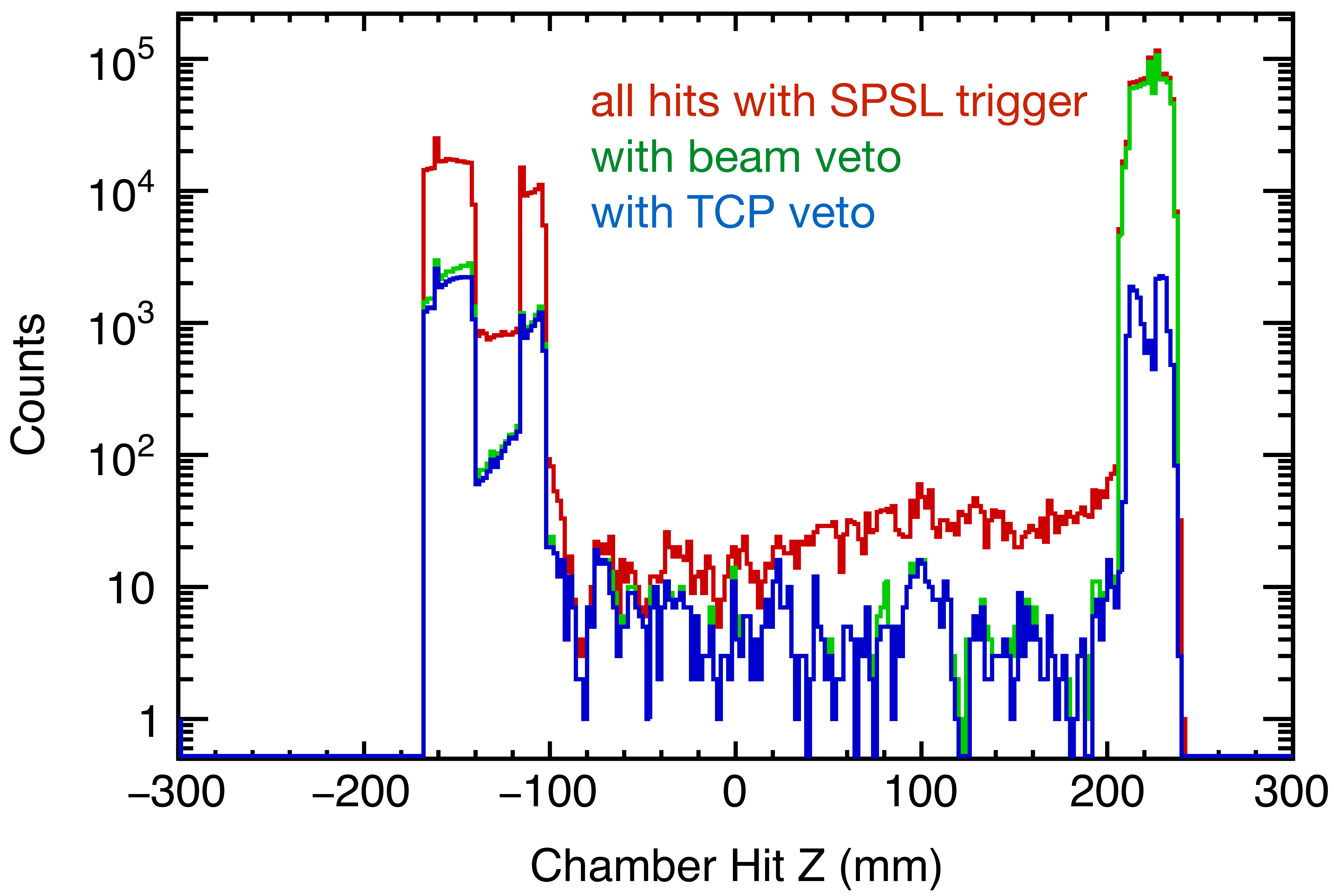

Planned simulation geometry update

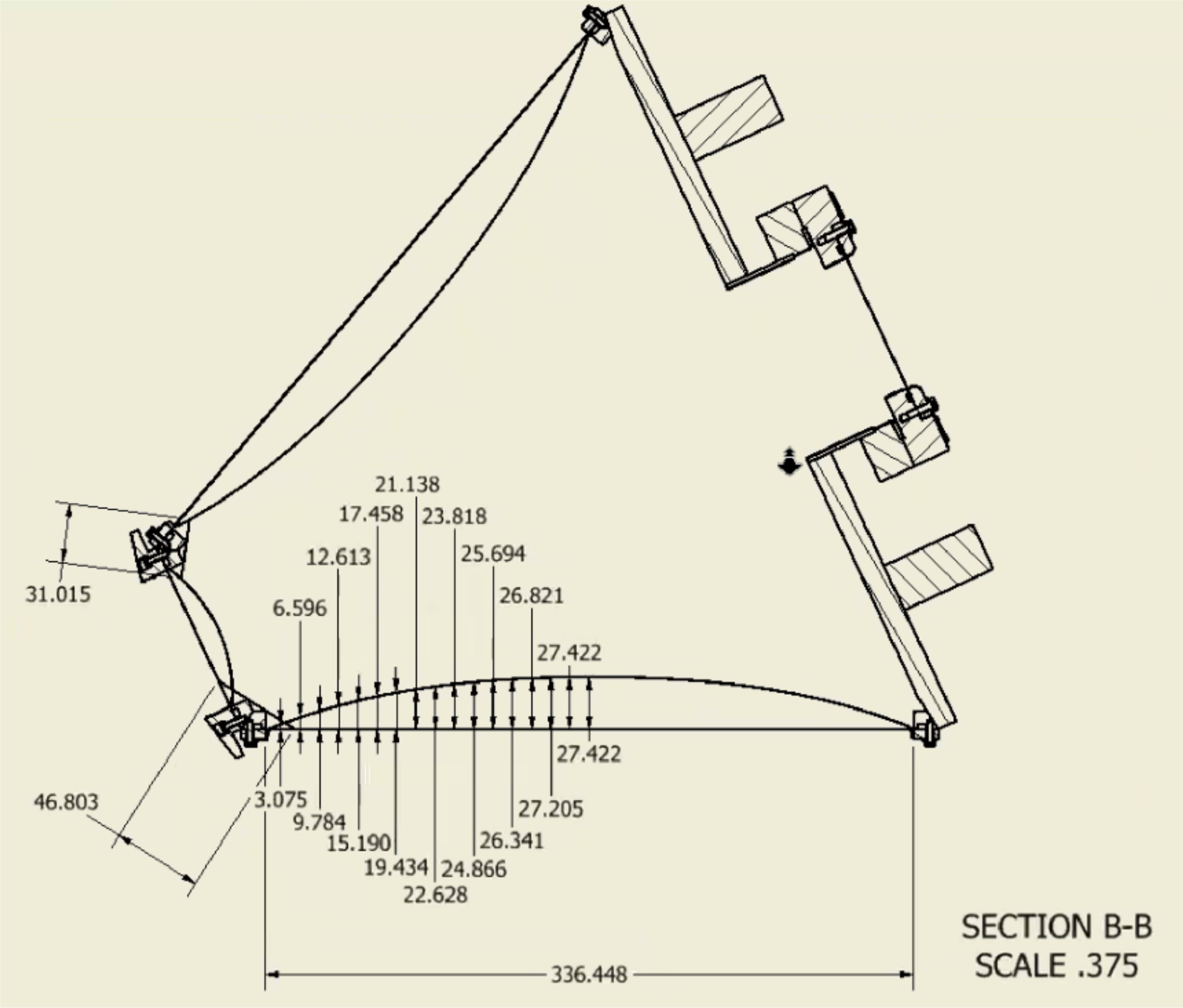

Drawing by Tom O'Connor (ANL)

The chamber windows bow inwards when the chamber is under vacuum

A more realistic shape of the side-exit window is needed in the simulation to properly simulate the correct **material thickness for all scattering angles**.

Detector positions in the simulation define the geometry used in the data analysis

- Implement the geometry consistent with design or known as-built geometry

↓

- Survey the setup
- Modify geometry of simulation to fit survey data

↓

- Export geometry as GDML file for use in data analysis

Example fit result

```
/g4PSI/det/trans GEM0    -0.511     0.106    -0.008 mm
/g4PSI/det/trans GEM1    -1.034     1.020    -4.803 mm
/g4PSI/det/trans GEM2    -0.754     0.246     0.937 mm
/g4PSI/det/trans GEM3    -1.151     0.304     0.065 mm

/g4PSI/det/rot GEM0     0.036     0.018    -0.541 deg
/g4PSI/det/rot GEM1    -0.666    -0.233    -6.706 deg
/g4PSI/det/rot GEM2    -0.075     1.132    -1.290 deg
/g4PSI/det/rot GEM3     0.032    -0.164    -0.223 deg
```

fit translational and rotational offsets

Modeling the particle beam

- Particle mix
- Position and direction distributions including (new) correlations

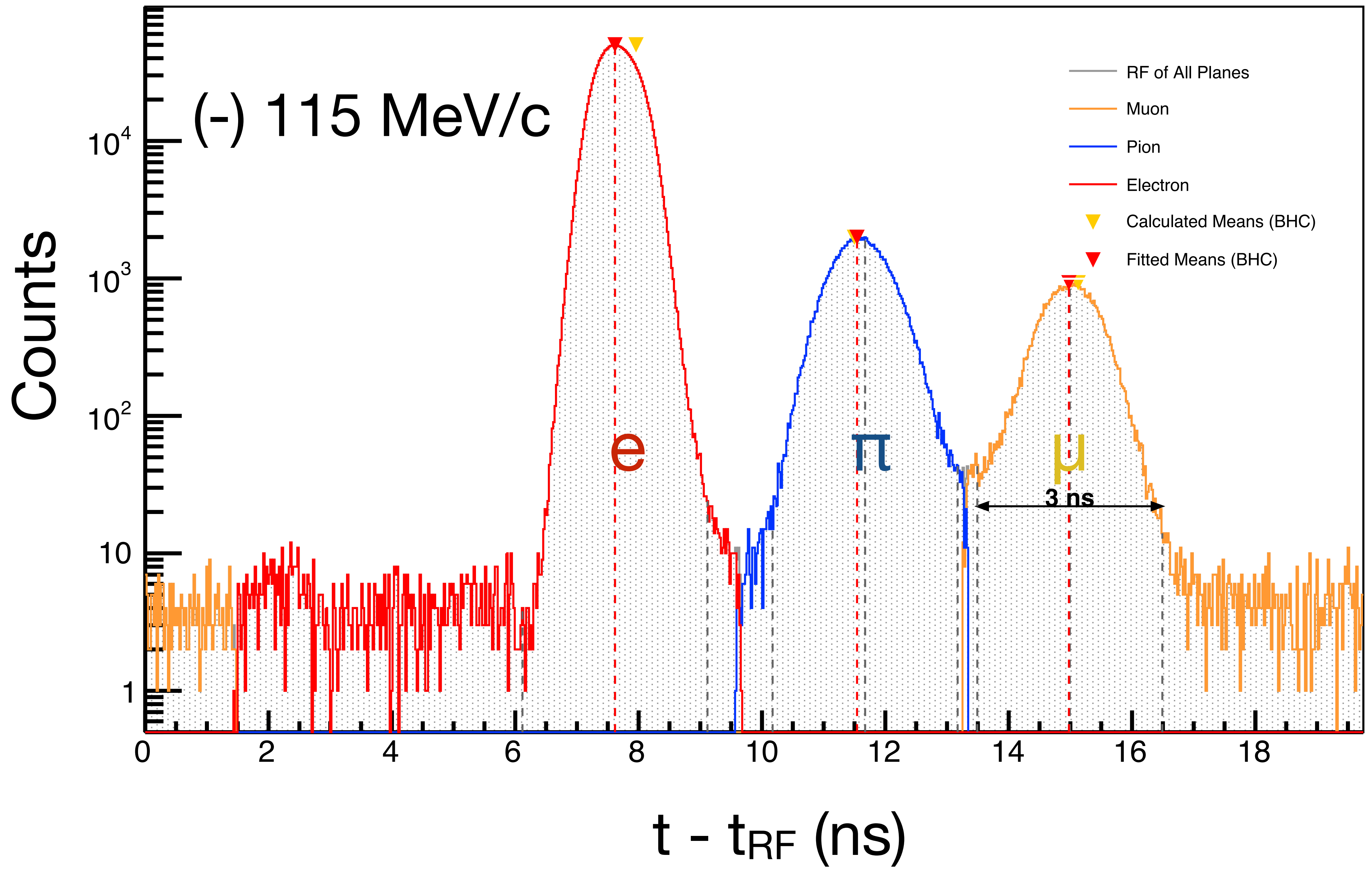

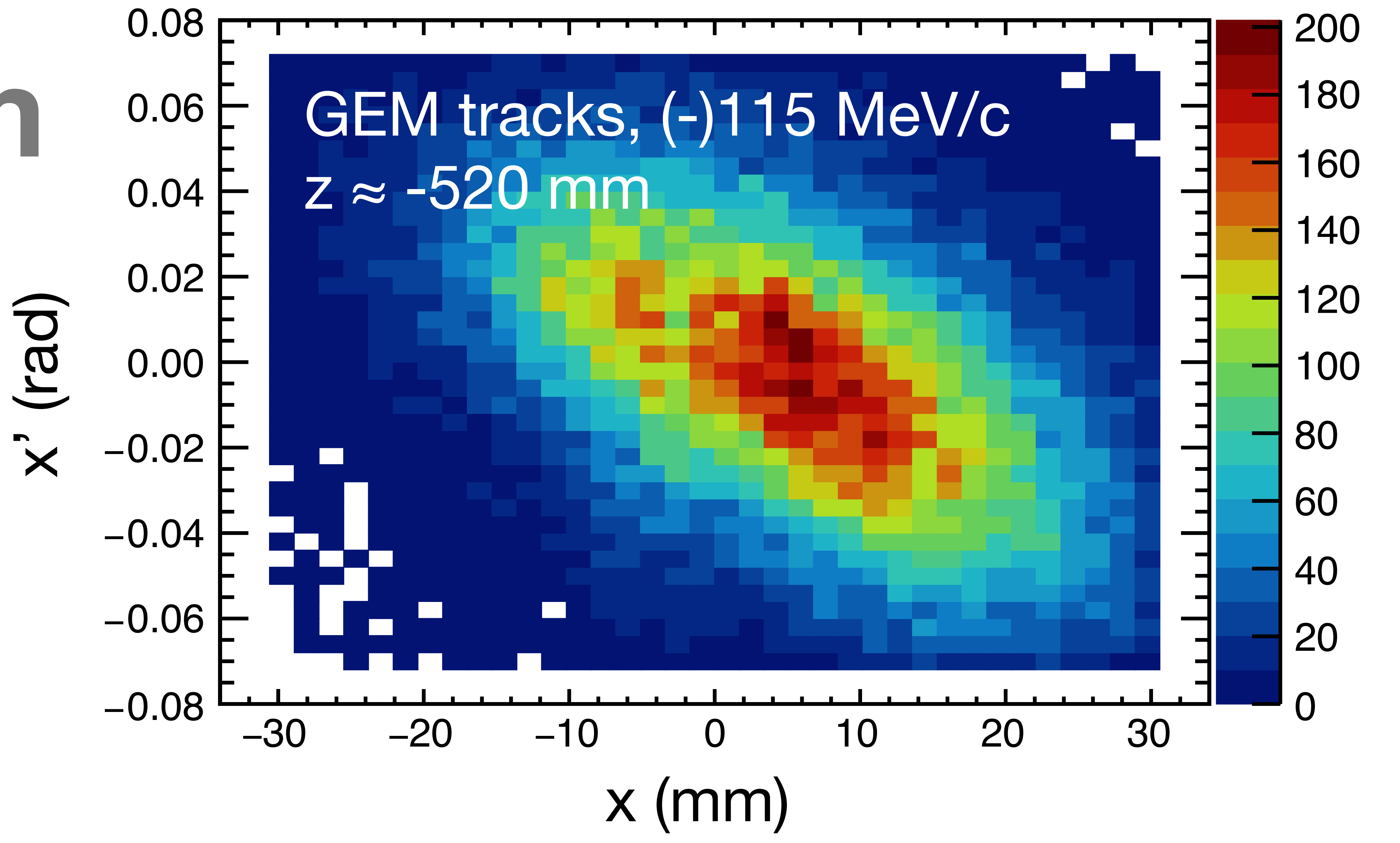

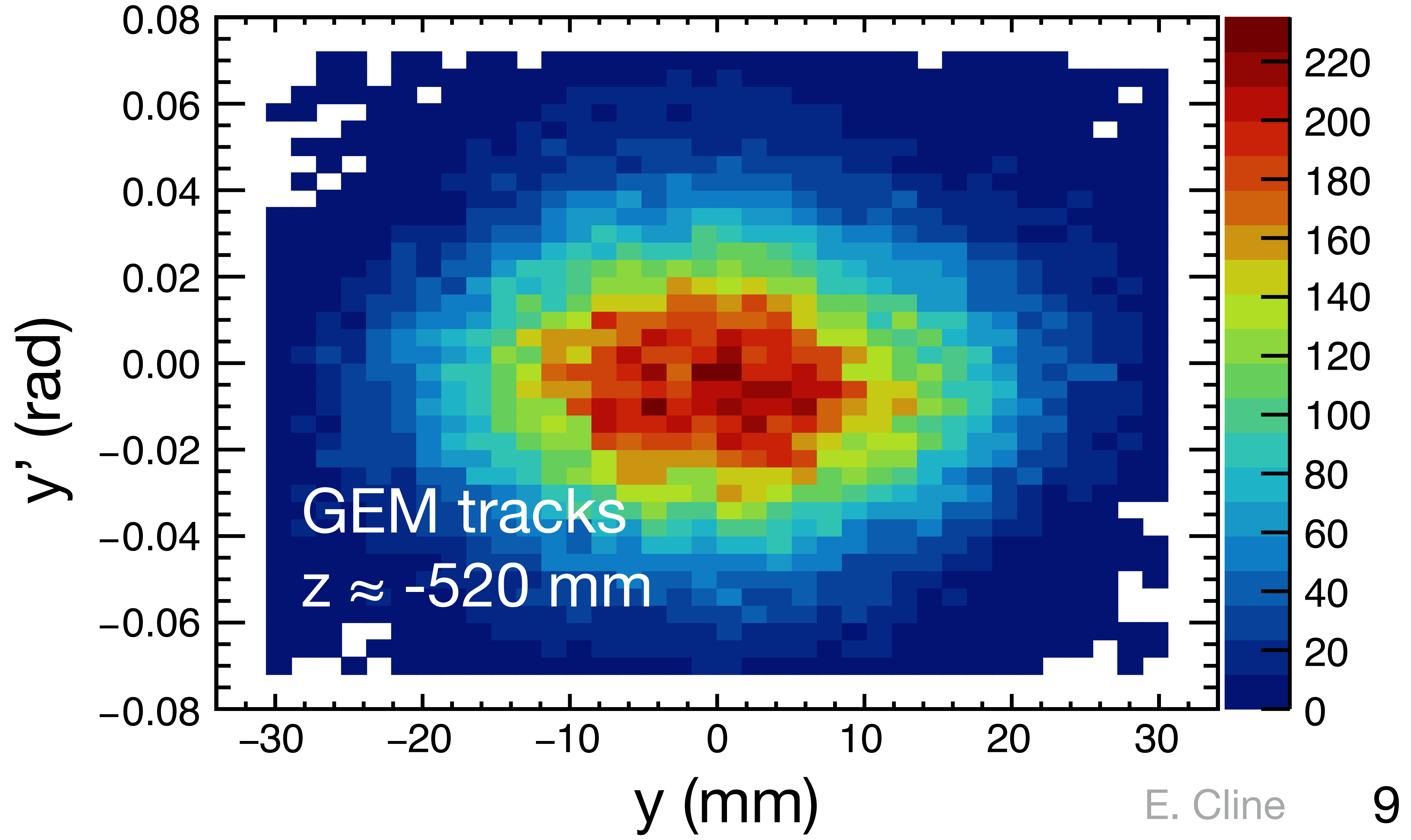

g4PSI Beam parameter tune to GEM-track distribution

Beam direction in y
(Simulation and data)

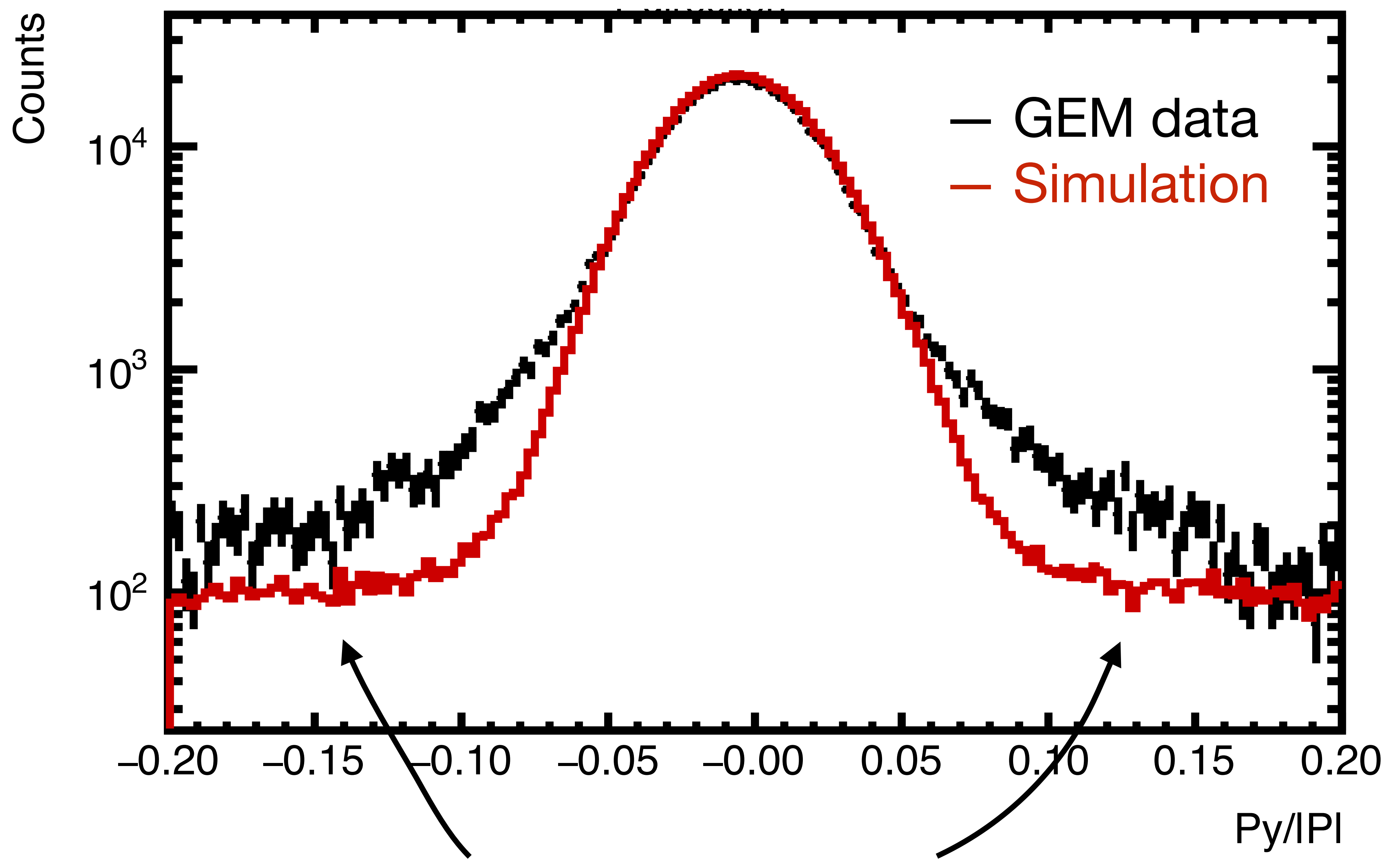

Tails from secondary particles

Correlation of beam direction and position along x (Simulation)

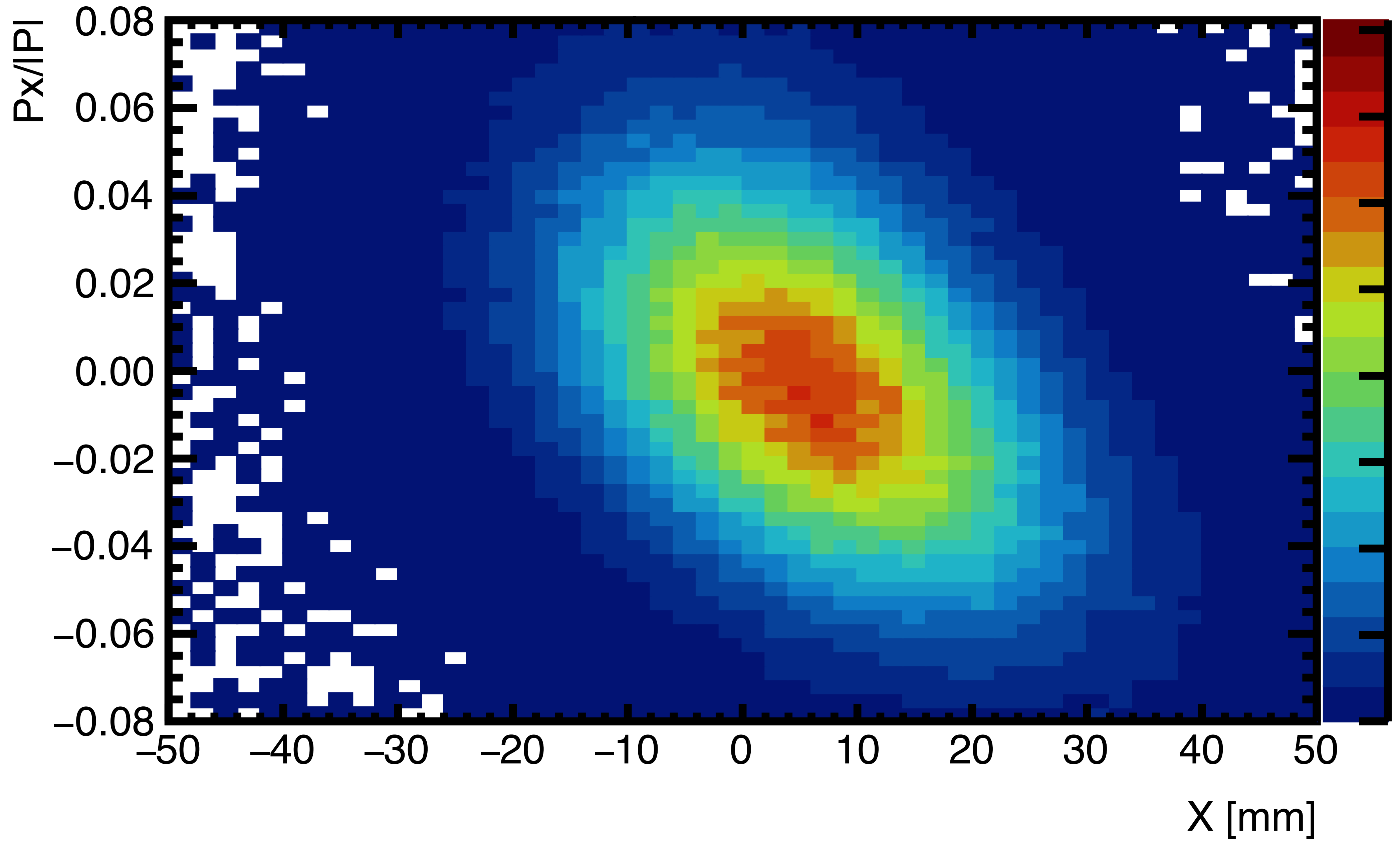

M. Nicol

Presently, all beam particle types in the simulation are assumed to have the same distributions.

All simulated detector responses are now digitized for analysis

Detectors	g4PSI	Digitization
SPS, BM, BH, VETO	g4PSIScintillatorSD	✓
CAL	g4PSICherenkovSD	✓
GEM	g4PSITrackerSD	✓
STT	g4PSITrackerSD	✓

Digitization of a simulated energy deposition of *E* at position *x* in a scintillator

SPS Examples

Digitized light output at the two PMTs:

$$Q_1(E,x) = g_1 E A_1(x)$$
$$Q_2(E,x) = g_2 E A_2(L-x)$$

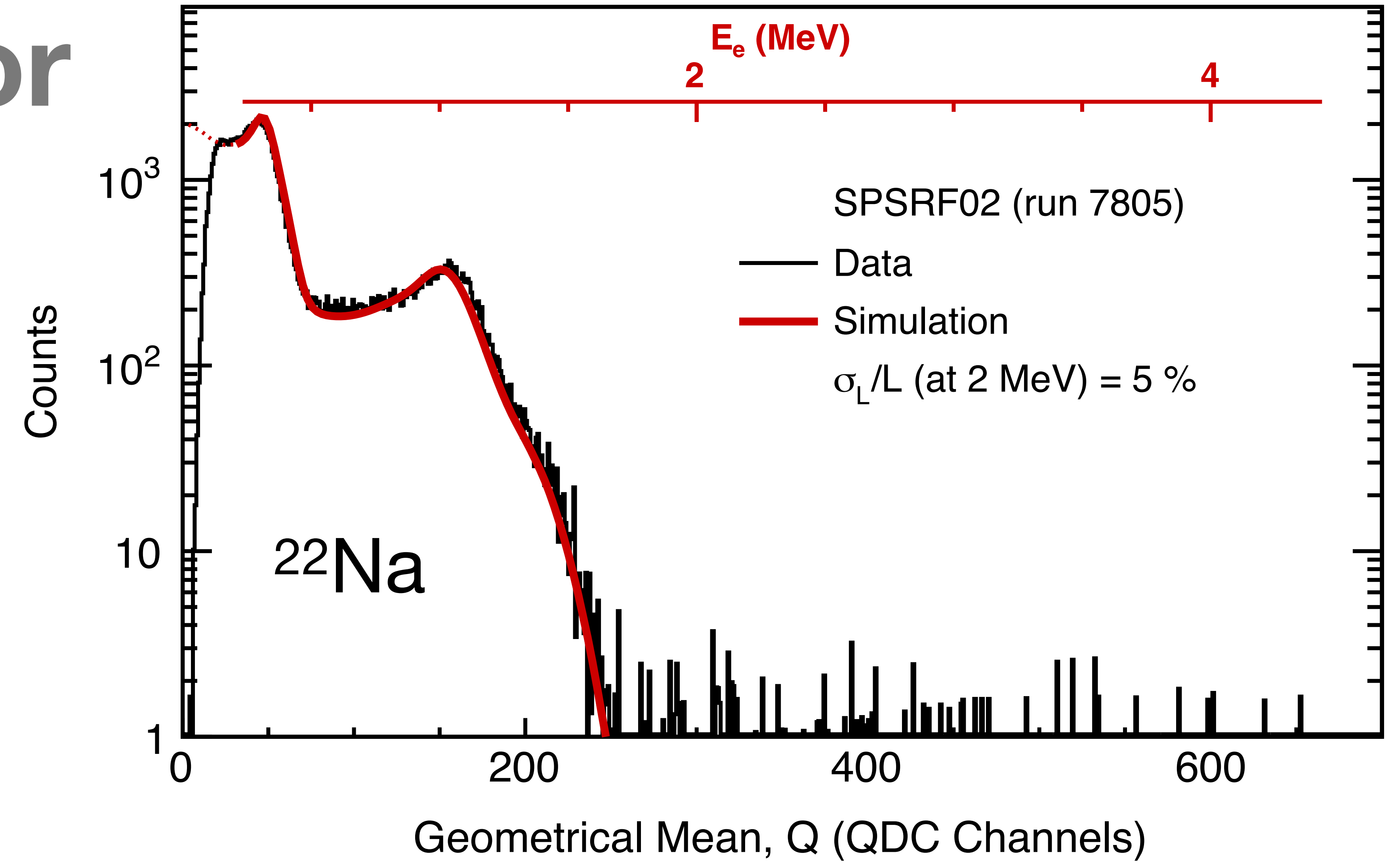

Detector characteristics that enter the digitization

- Pedestals
- Gains and light-output resolution
- Attenuation function, $A(L/2) = 1$
- Effective speed of light
- Time-walk correction
- Time resolution
- Discriminator threshold

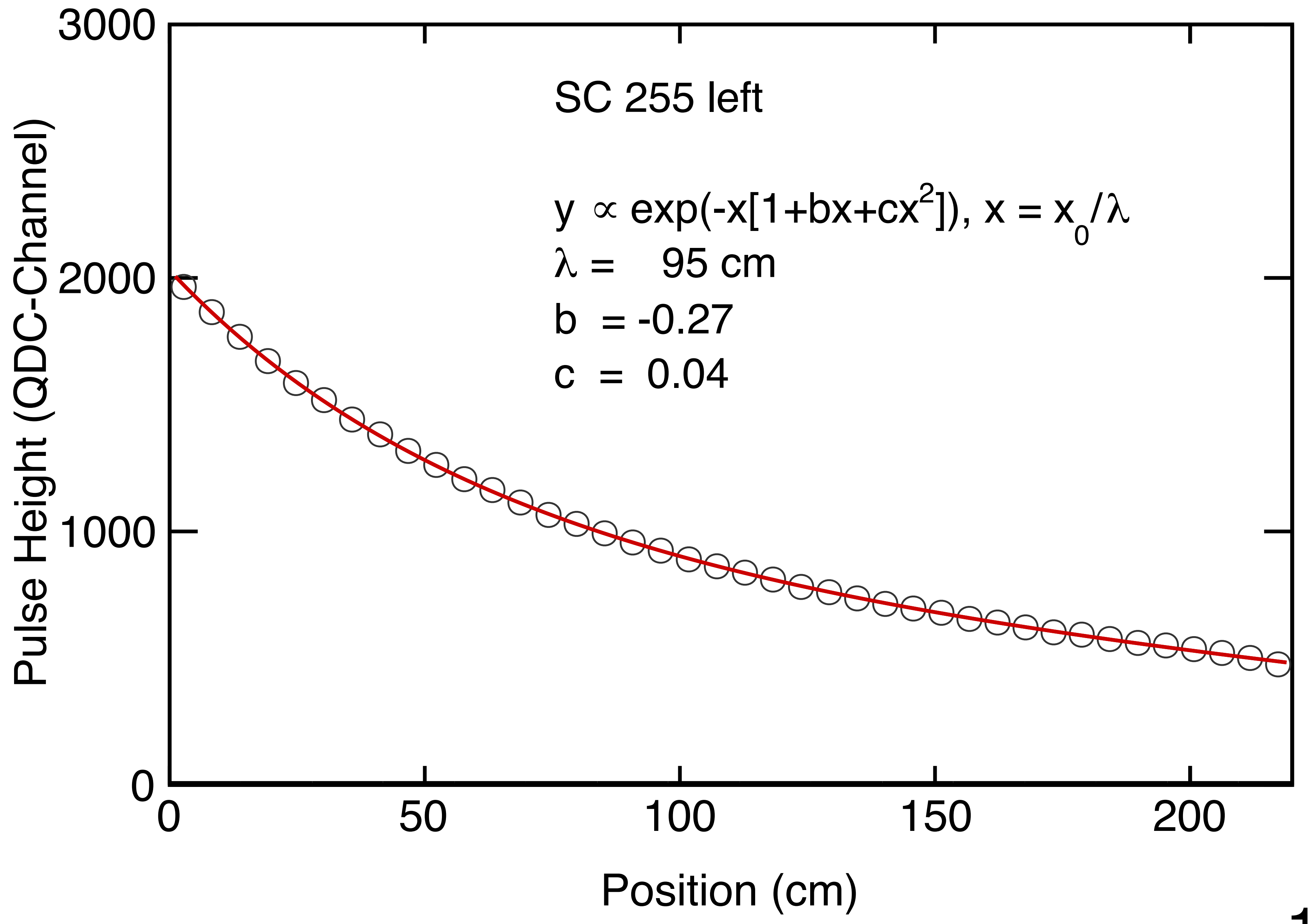

^{88}Y calibration to test detector response and simulation close to threshold

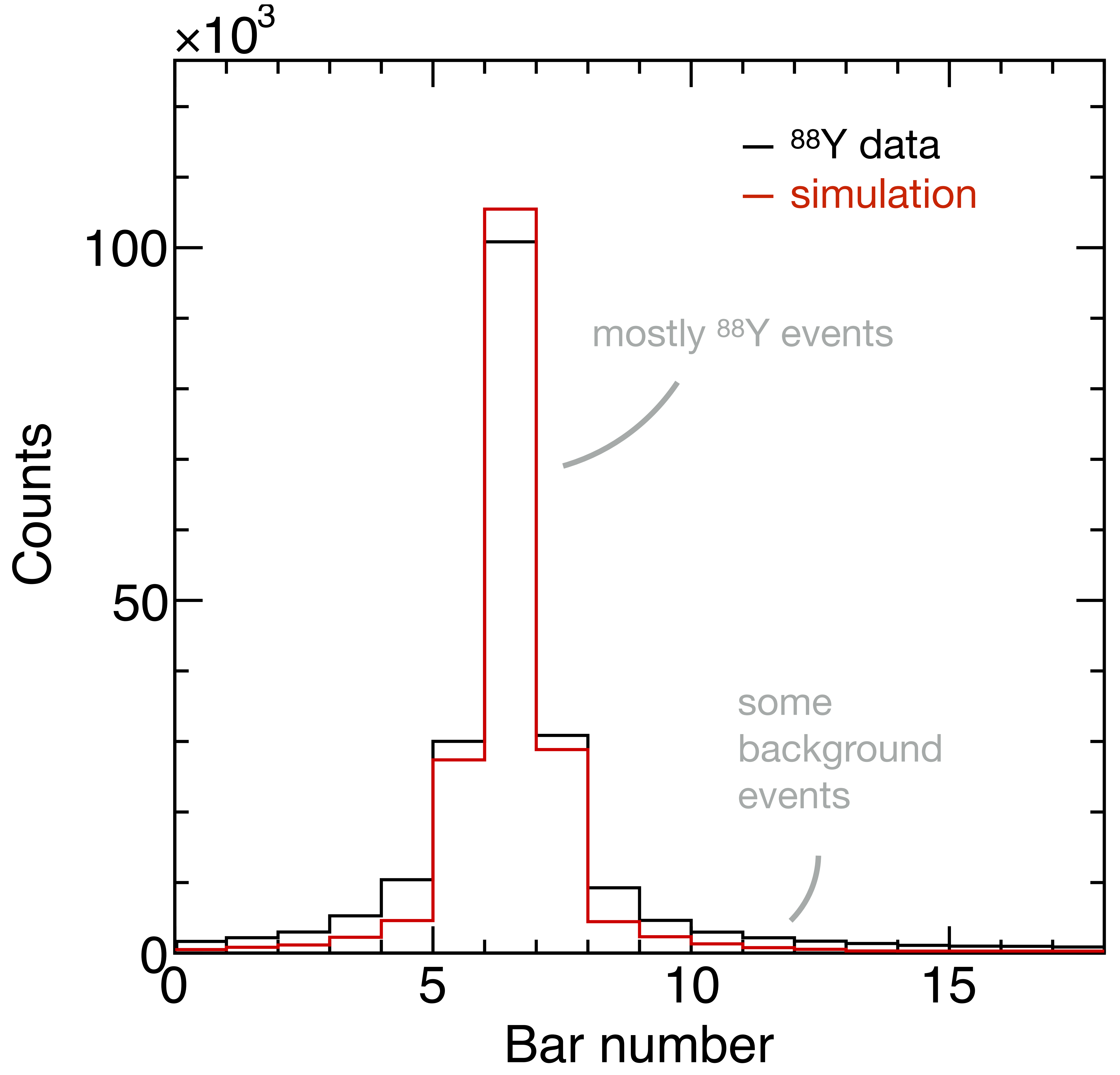

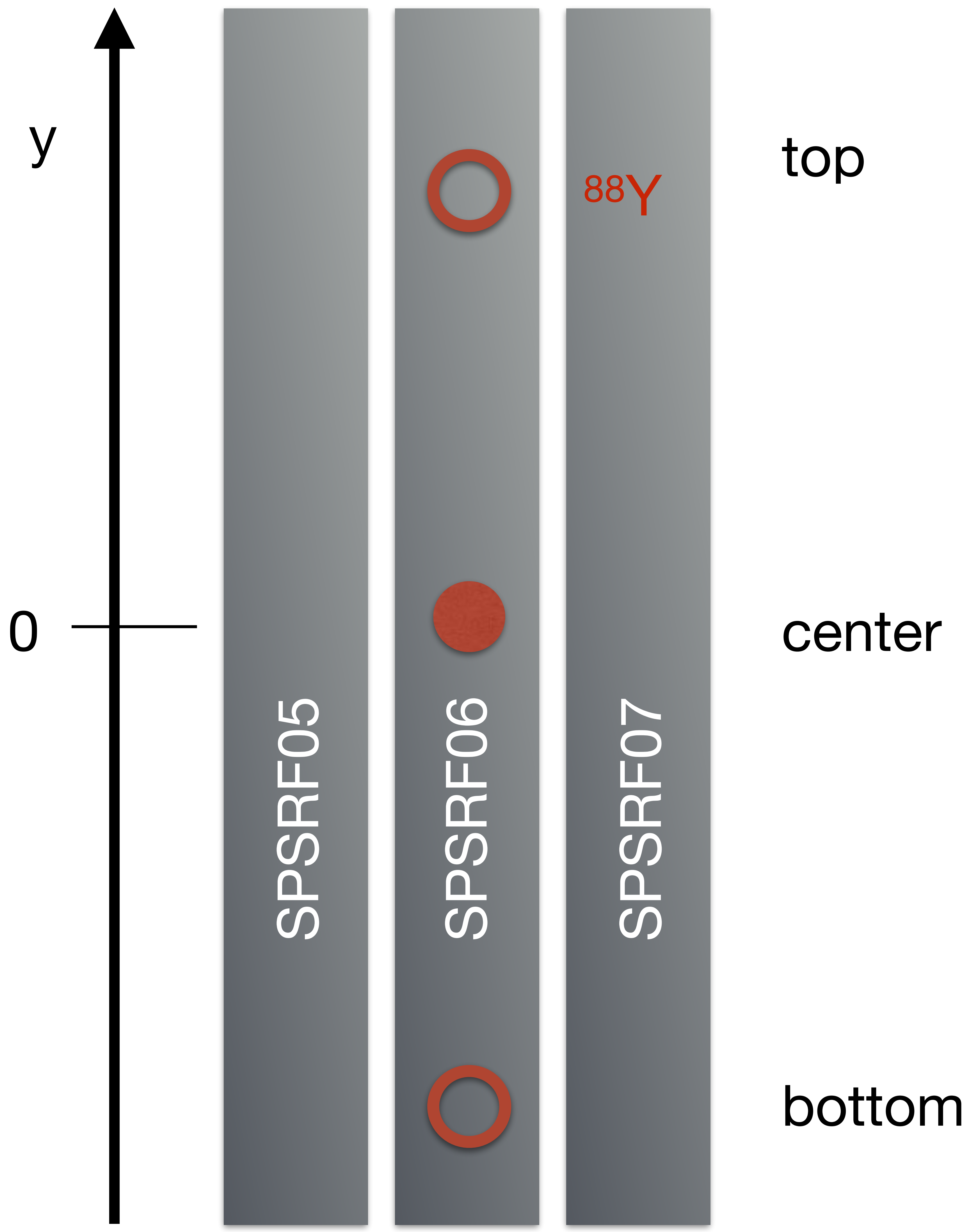

A. Flannery

Simulated time response, $\Delta t = t_{down} - t_{up}$

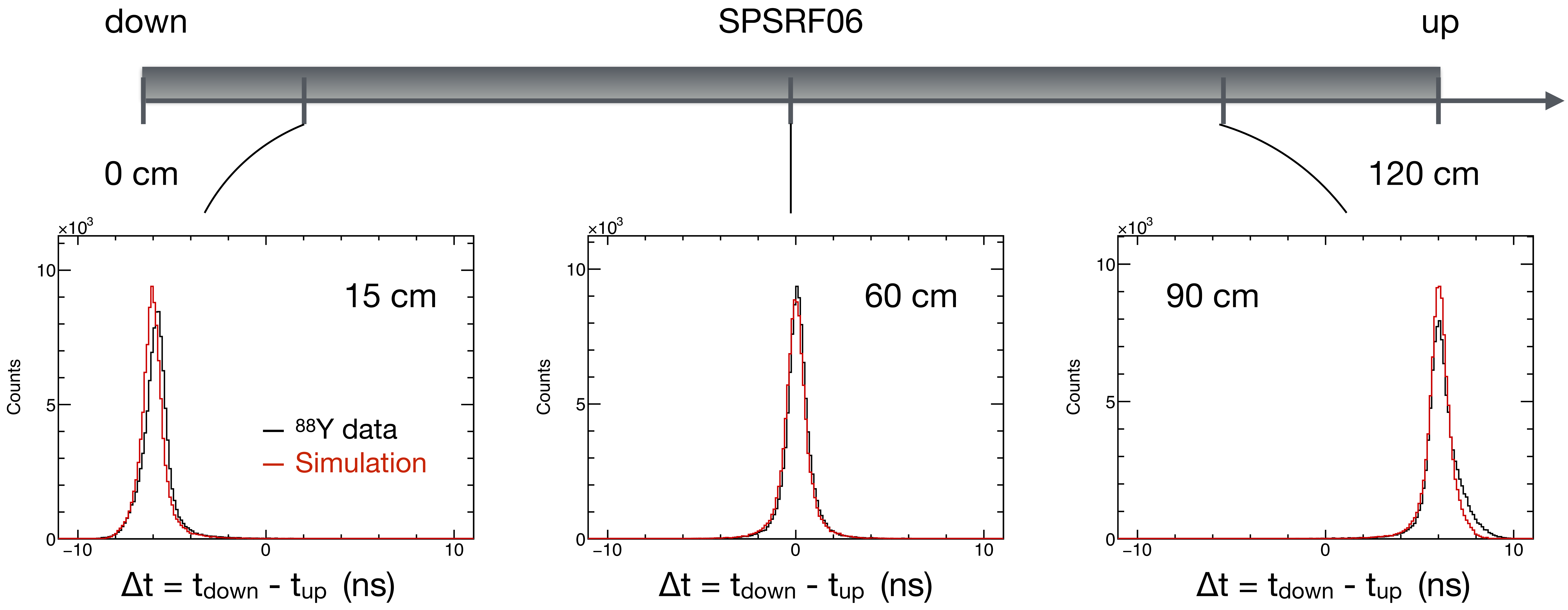

$$\Delta t = t_{\text{down}} - t_{\text{up}} = \frac{1}{c_{\text{eff}}}(2x - L)$$

Effective speed of light: $c_{eff} \approx 14.5$ cm / ns

Simulated light output and attenuation

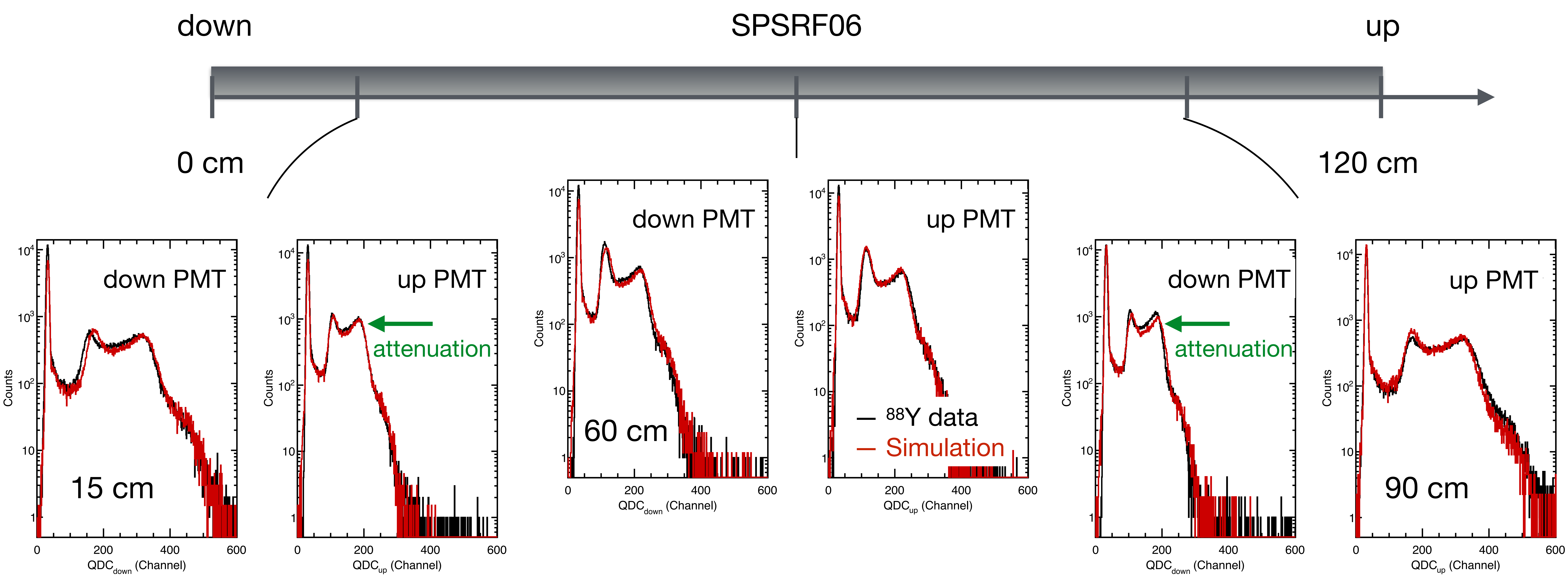

The pedestal to signal ratio and the below-threshold events are properly described by the simulation when the trigger on the SPSRF wall is considered.

BH

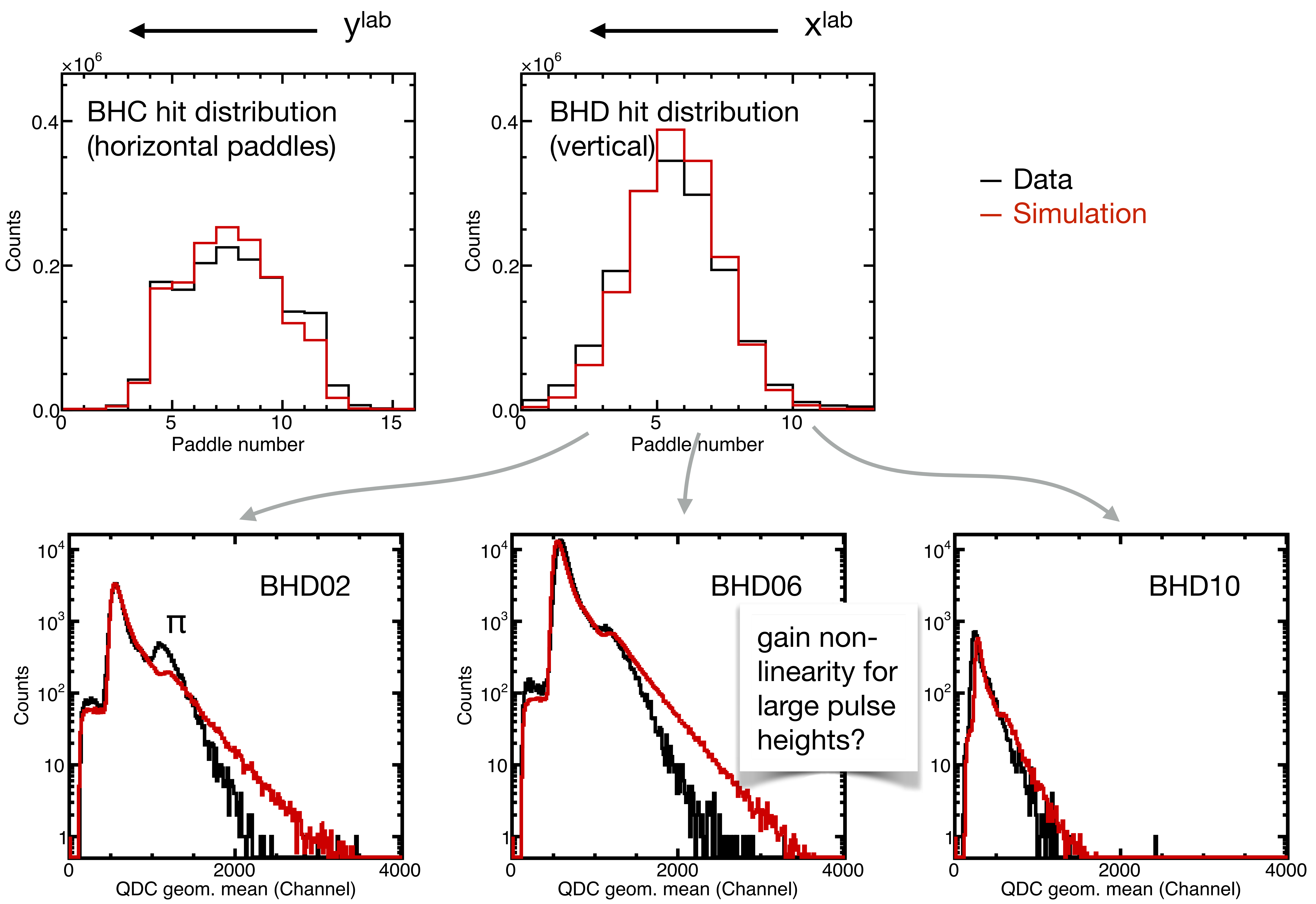

relatively more pions in the data at the low-momentum edge of the distribution

VETO

Larger variety of **energy depositions** in the experiment.

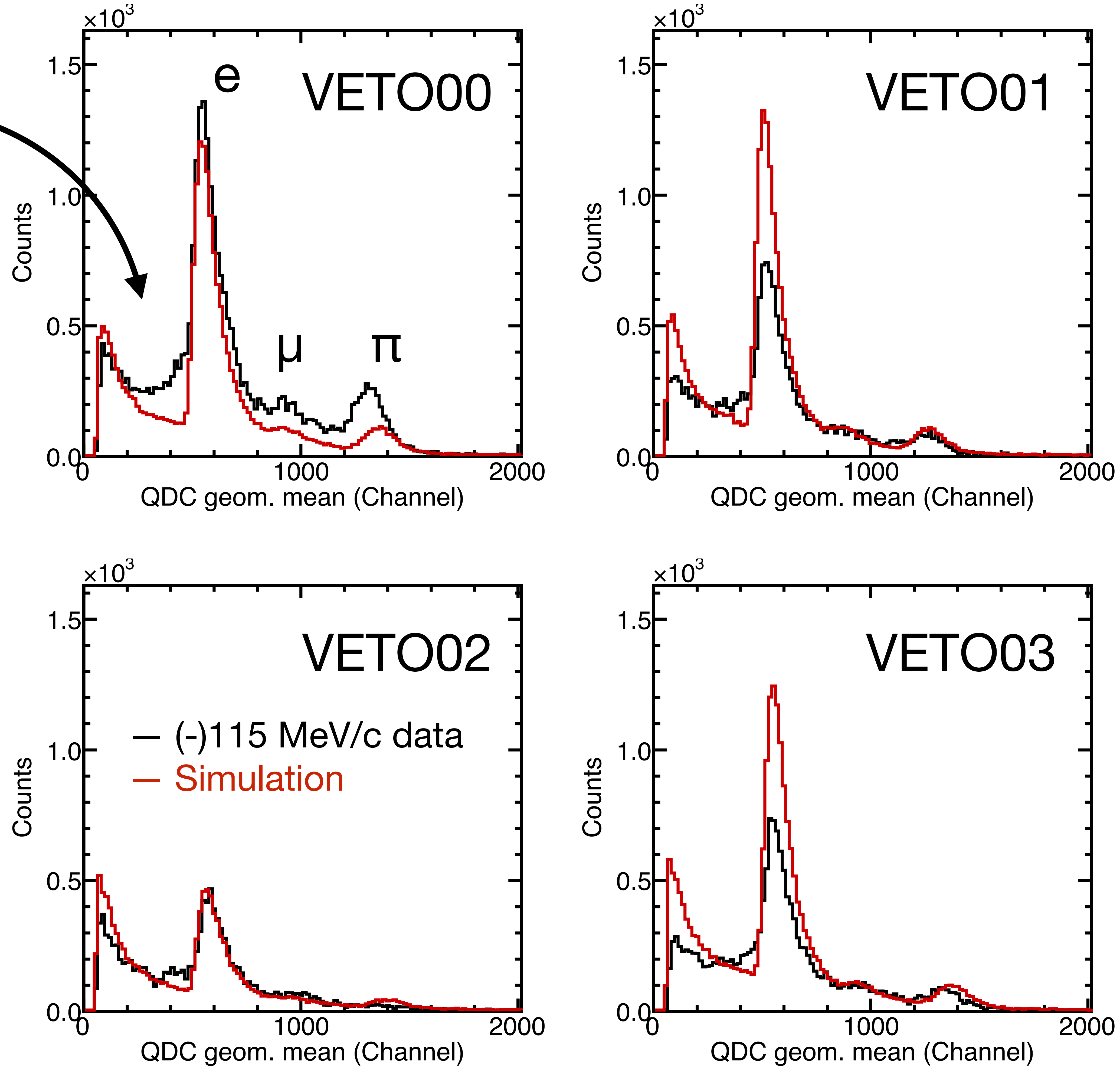

Yield fractions for various paddles are difficult to simulate:

- Beam tails
- Secondary particles

Particles hitting the VETO detector:

30% scattering-trigger events

VETO detector paddle

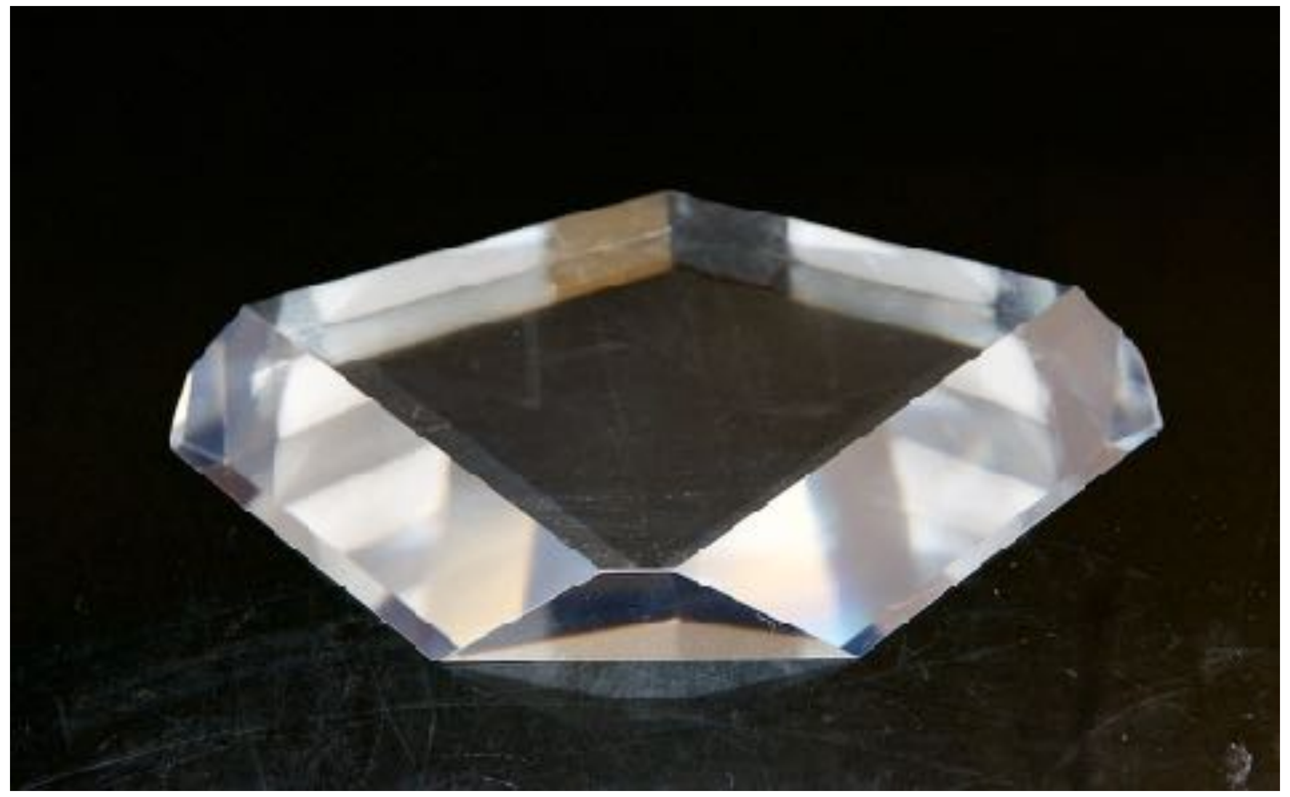

Simplified model of VETO detector paddle in the simulation.

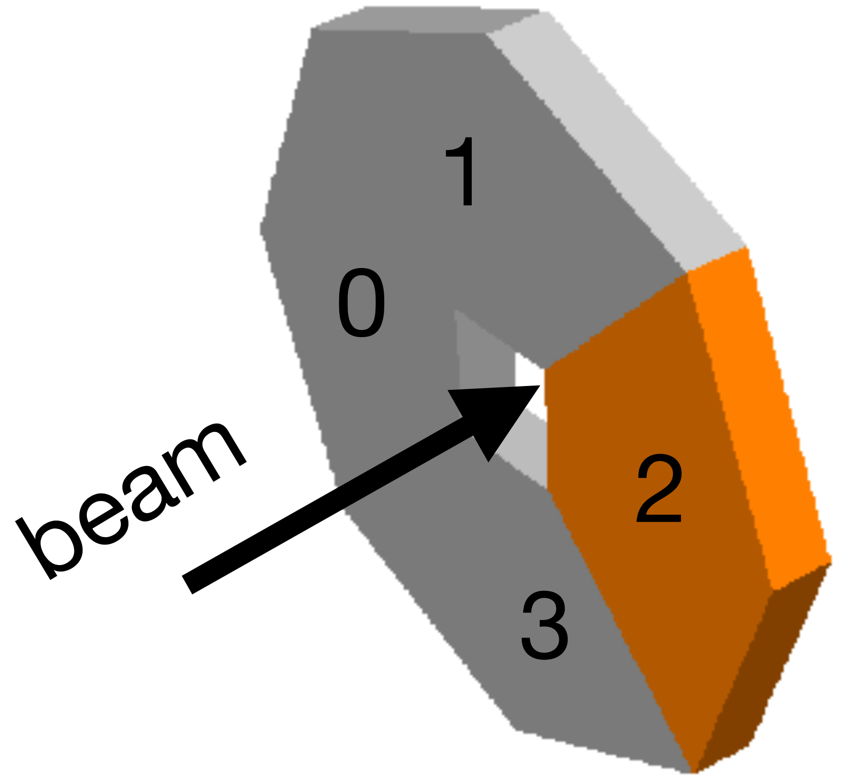

BM — Energy deposition

— (-)115 MeV/c data
— Simulation

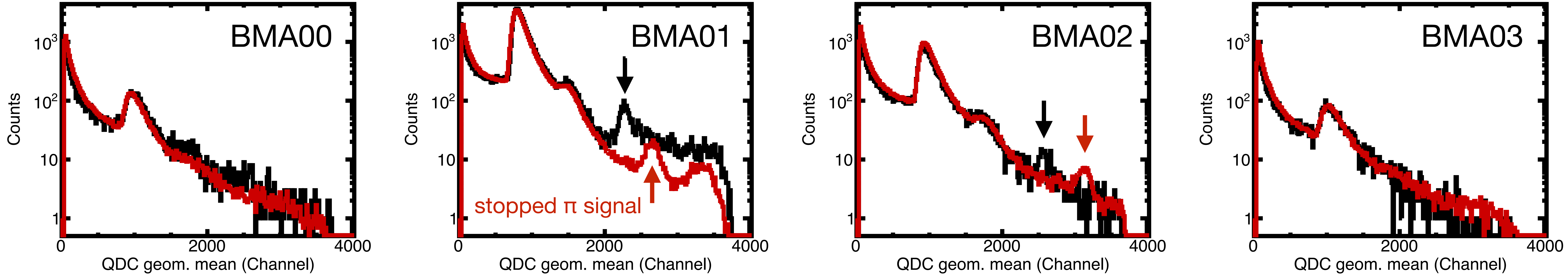

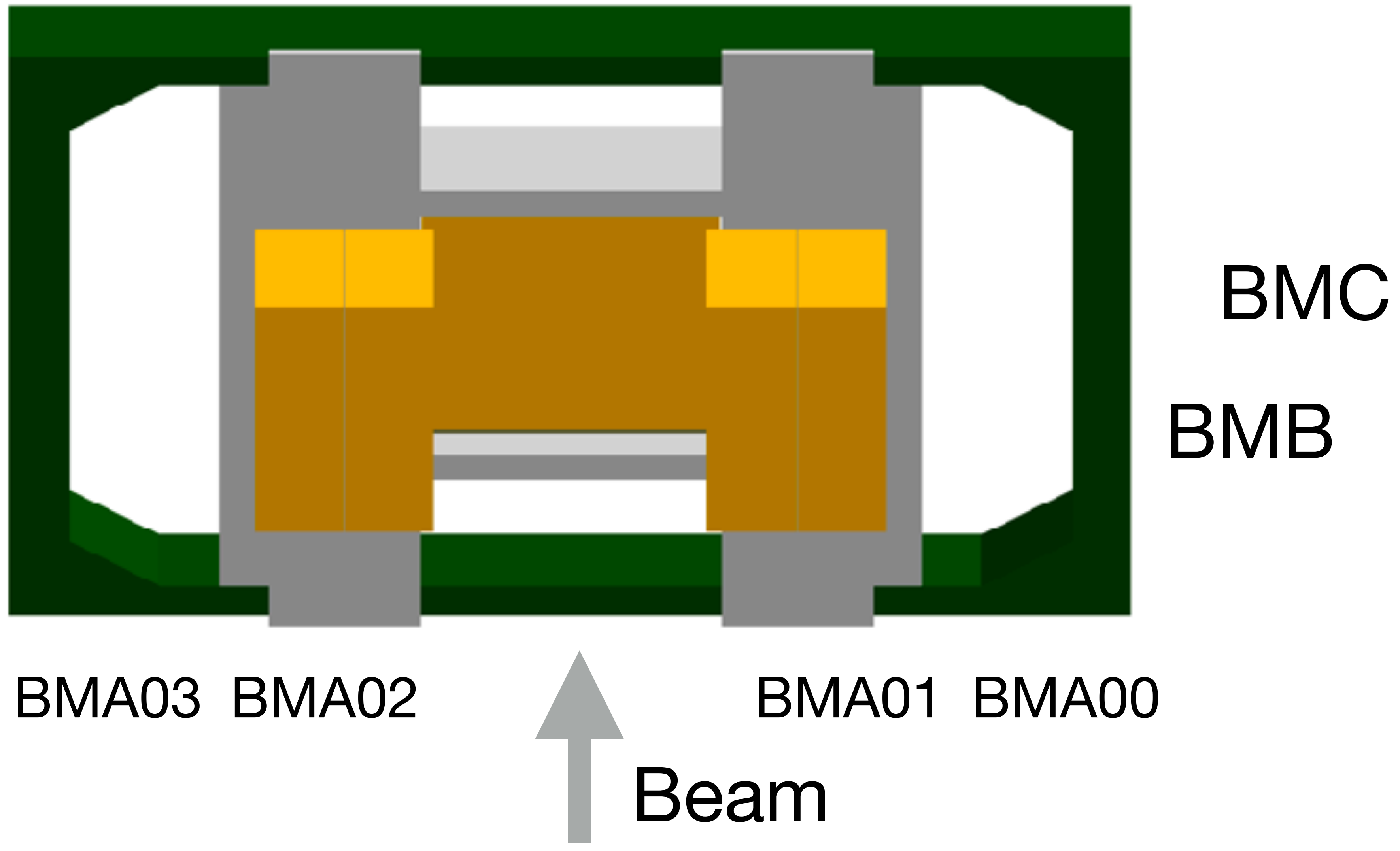

π stopped in the inner two BMA bars, but no evidence of pions reaching outer two BMA bars.

Excellent agreement for electron and muon energy depositions.

Mismatch of measured and simulated stopped-π energy deposition:

- gain non-linearity, saturation?
- too narrow integration gate?
- energy degradation of π not in the simulation?

Ionization quenching in the scintillators

Quenching function for BC-408

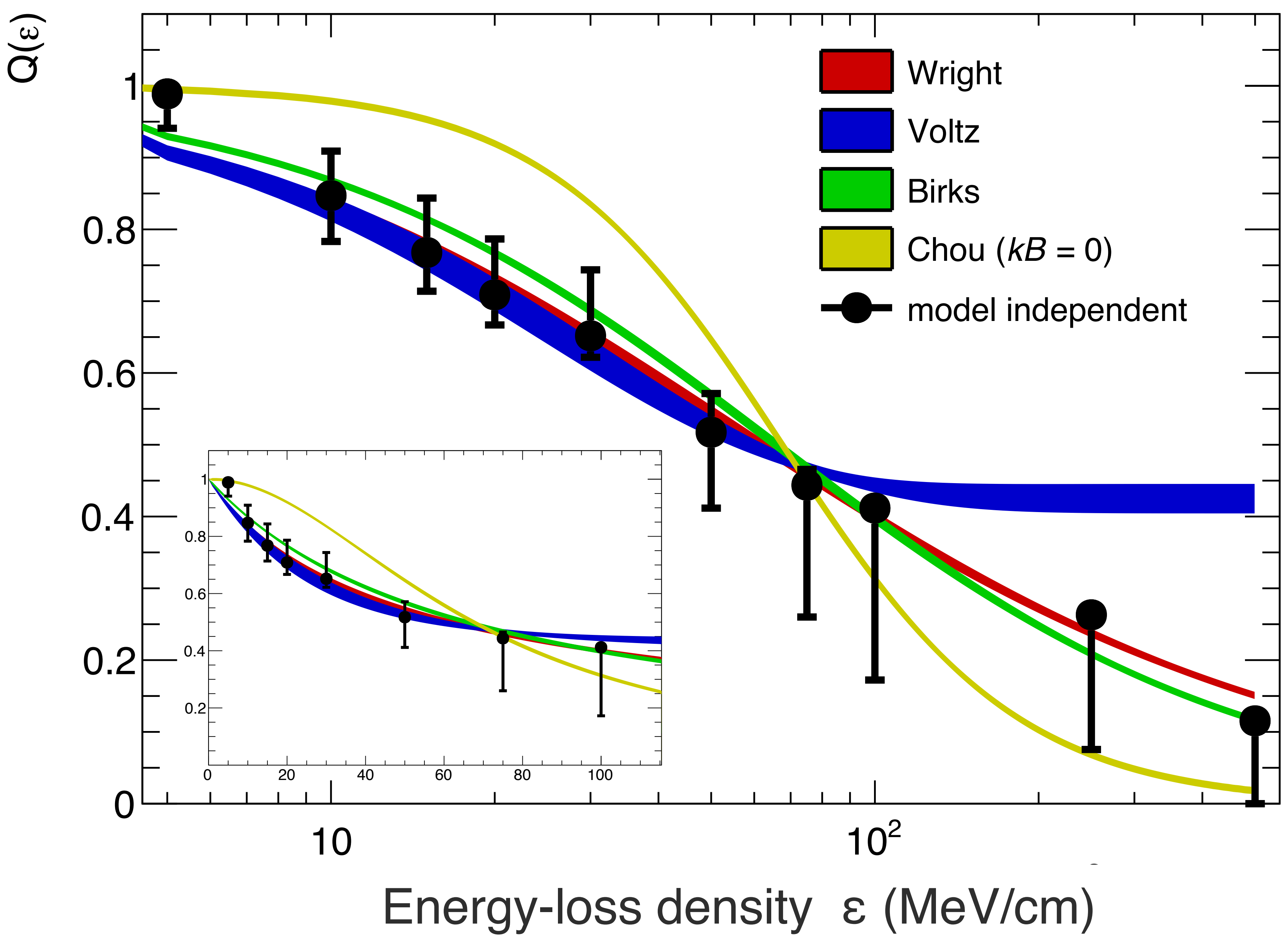

Th. Pöschel et al., NIM A 988, 164865 (2021)

- Ionization quenching is relevant for digitization
- Parameters need to be tuned for EJ-204

<u>Original</u>
No quenching in the digitization

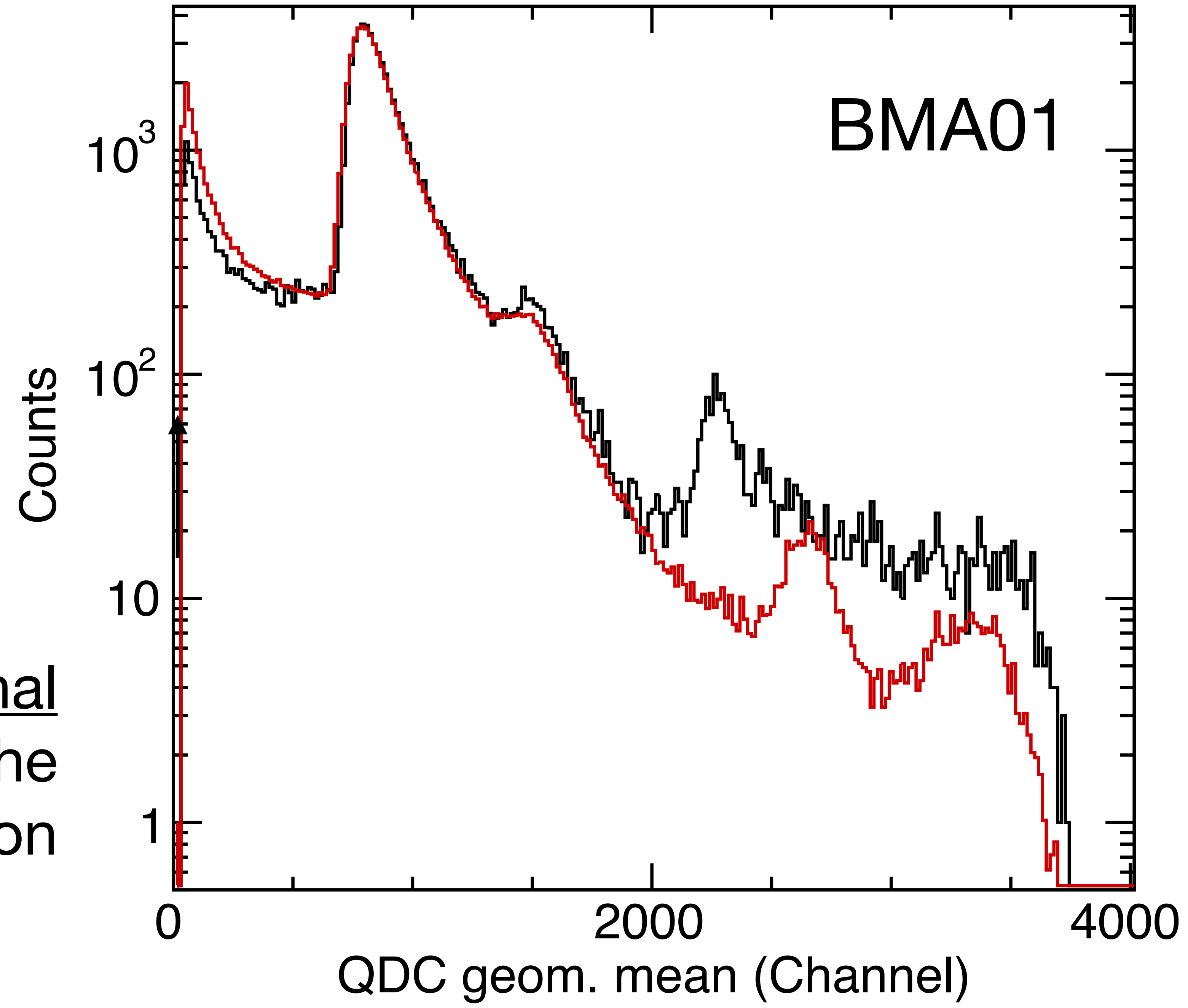

Including Wright quenching function for BC-408

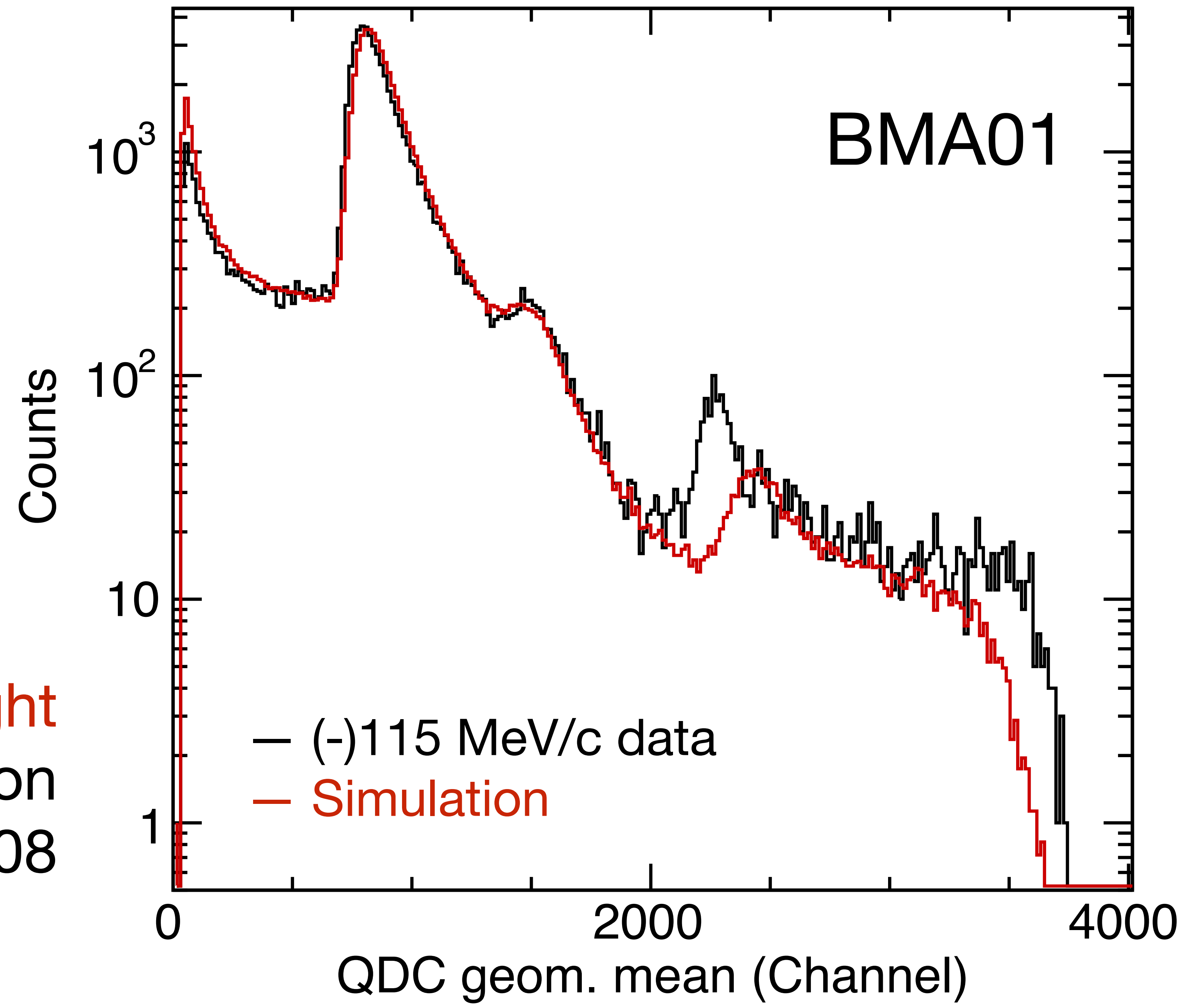

BM — Hit distributions well described

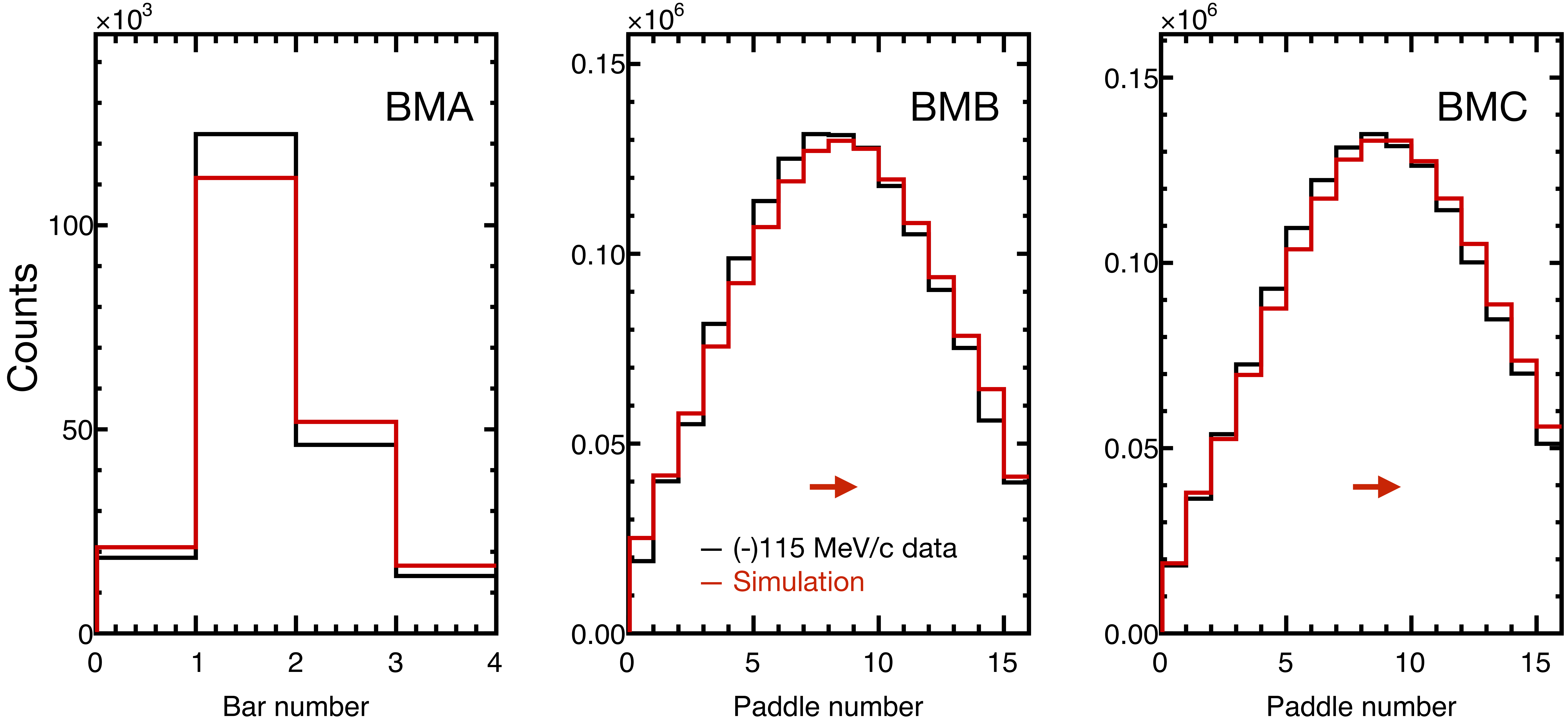

Tool to constrain beam parameterization for the simulation?

Simulated beam possibly shifted by 1/3 of a paddle width to larger paddle numbers (beam left), this corresponds to 2 mrad as seen from GEM0.

BM time resolution

BM read by constant-fraction discriminators

Nevertheless, the time-resolution can be improved with <u>additional time-walk corrections</u>

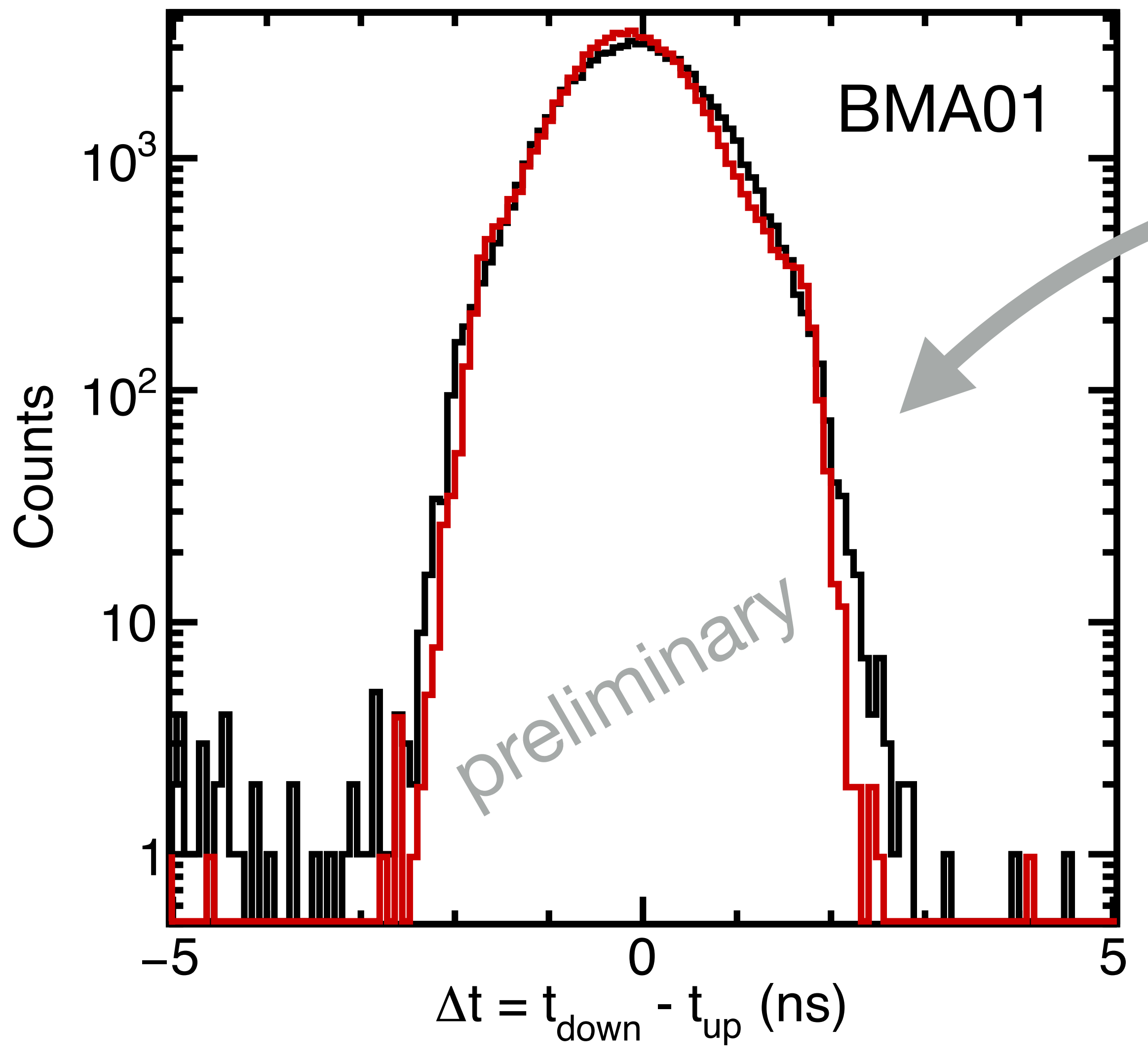

BMA: fair description with the assumed time resolution of $\sigma(t_{mean}) = 35$ ps

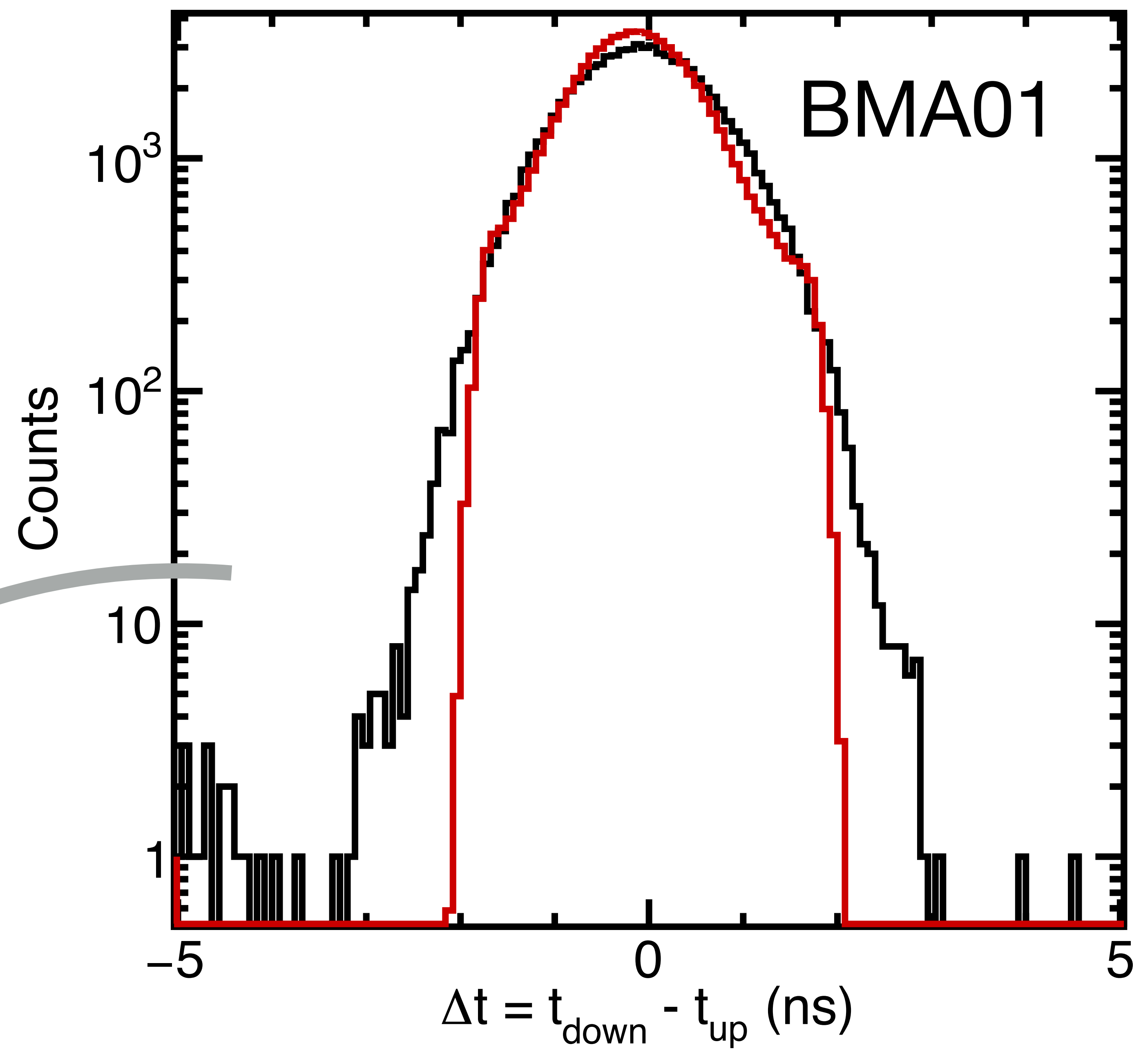

BMB, **BMC**: good description with the assumed time resolution of $\sigma(t_{mean}) = 100$ ps

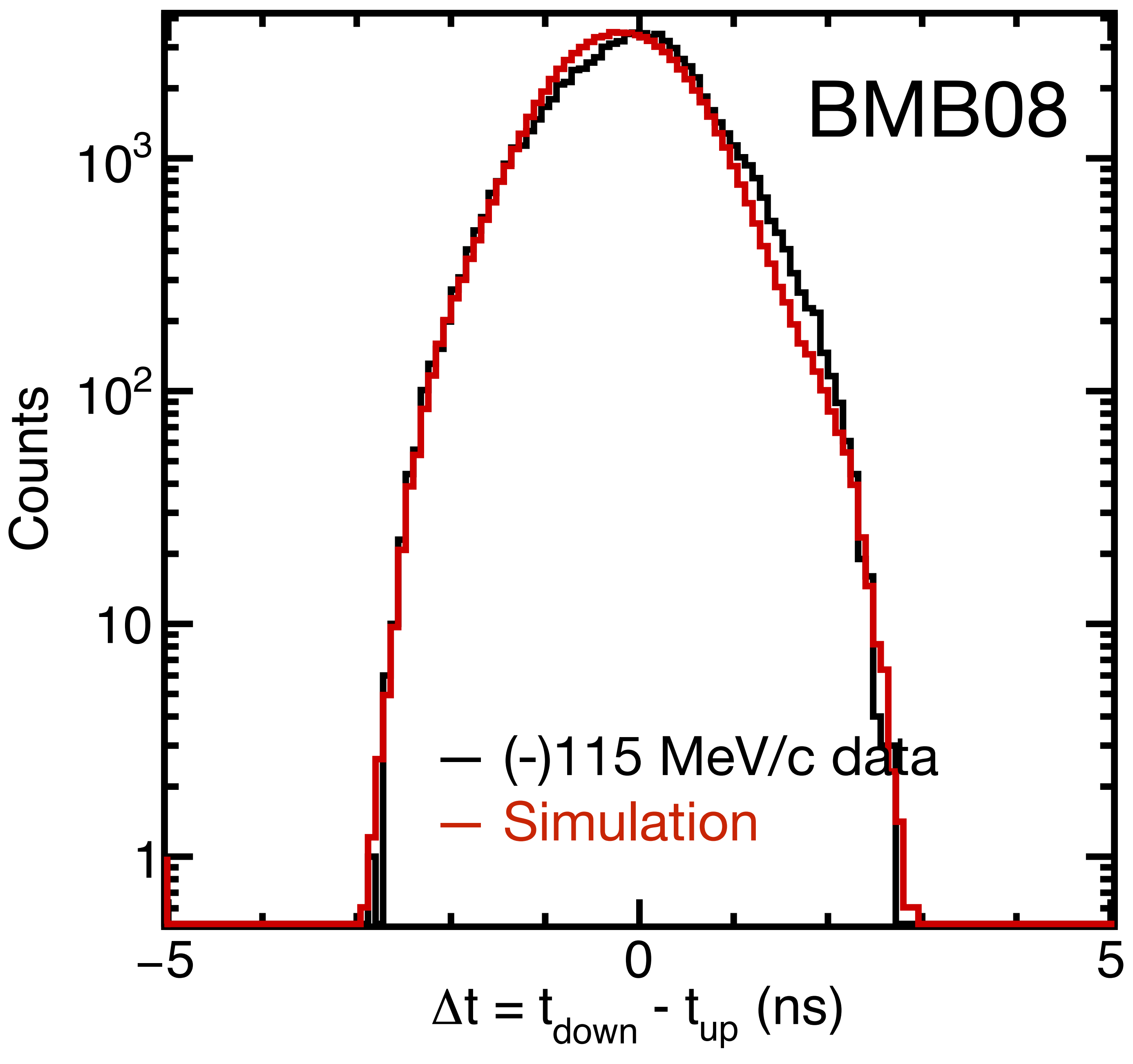

Expected width of the Δt distribution for 30-cm long scintillators: ± 2 ns

Simulation and digitization of lead-glass Cherenkov detector

Method A: Cherenkov light production and photon transport by Geant4. Accumulate photon yield, Y, at the site of the PMT.

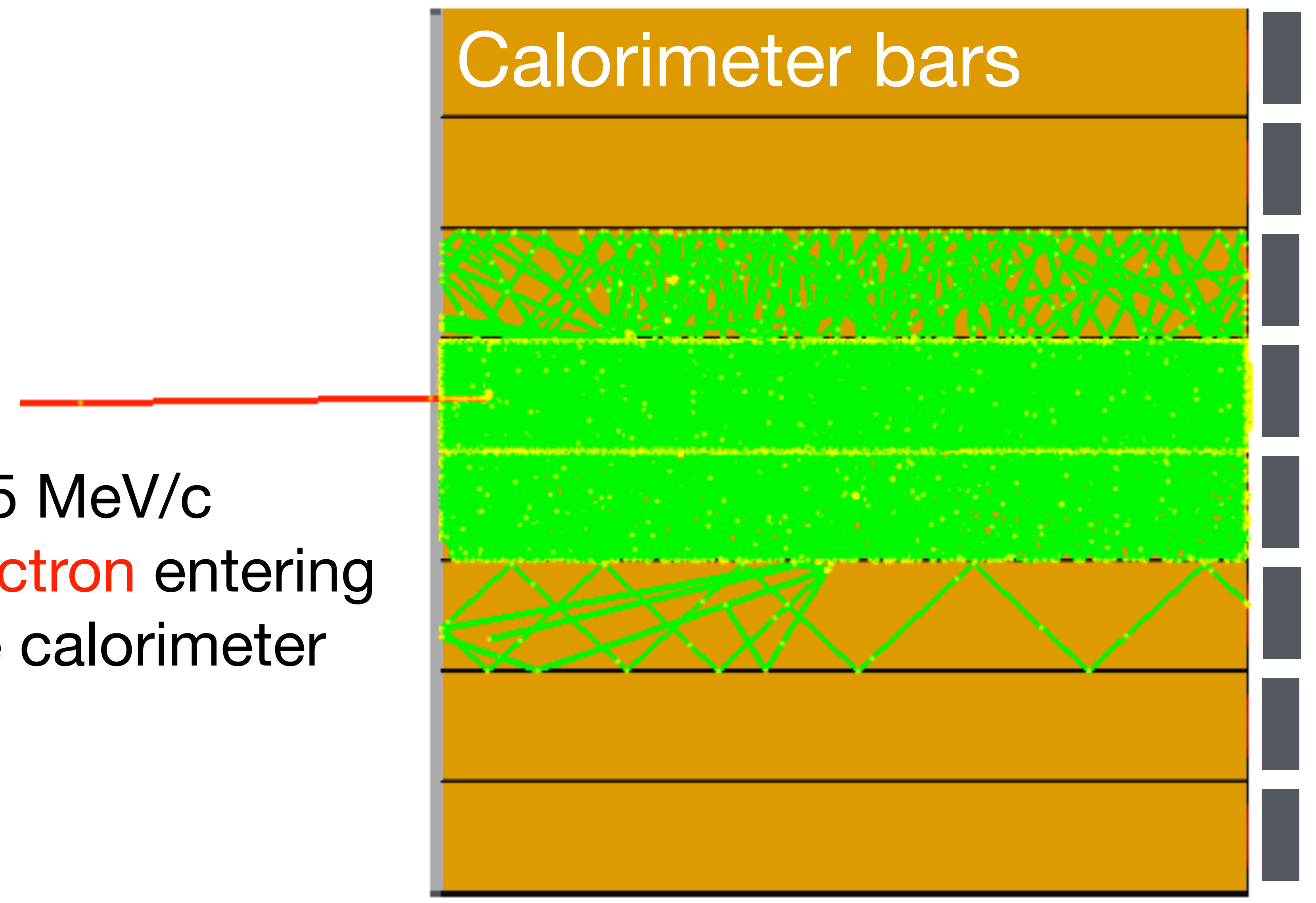

Photons in the block and total internal reflection

Method B (fast): Estimate the number of Cherekov photons from the speed of the particle:

$$Y \propto \int 1 - \frac{1}{n^2 \beta(x)^2}$$

Digitization: Conversion of light-output *Y* to QDC values (pedestal, gain per lead-glass element, resolution).

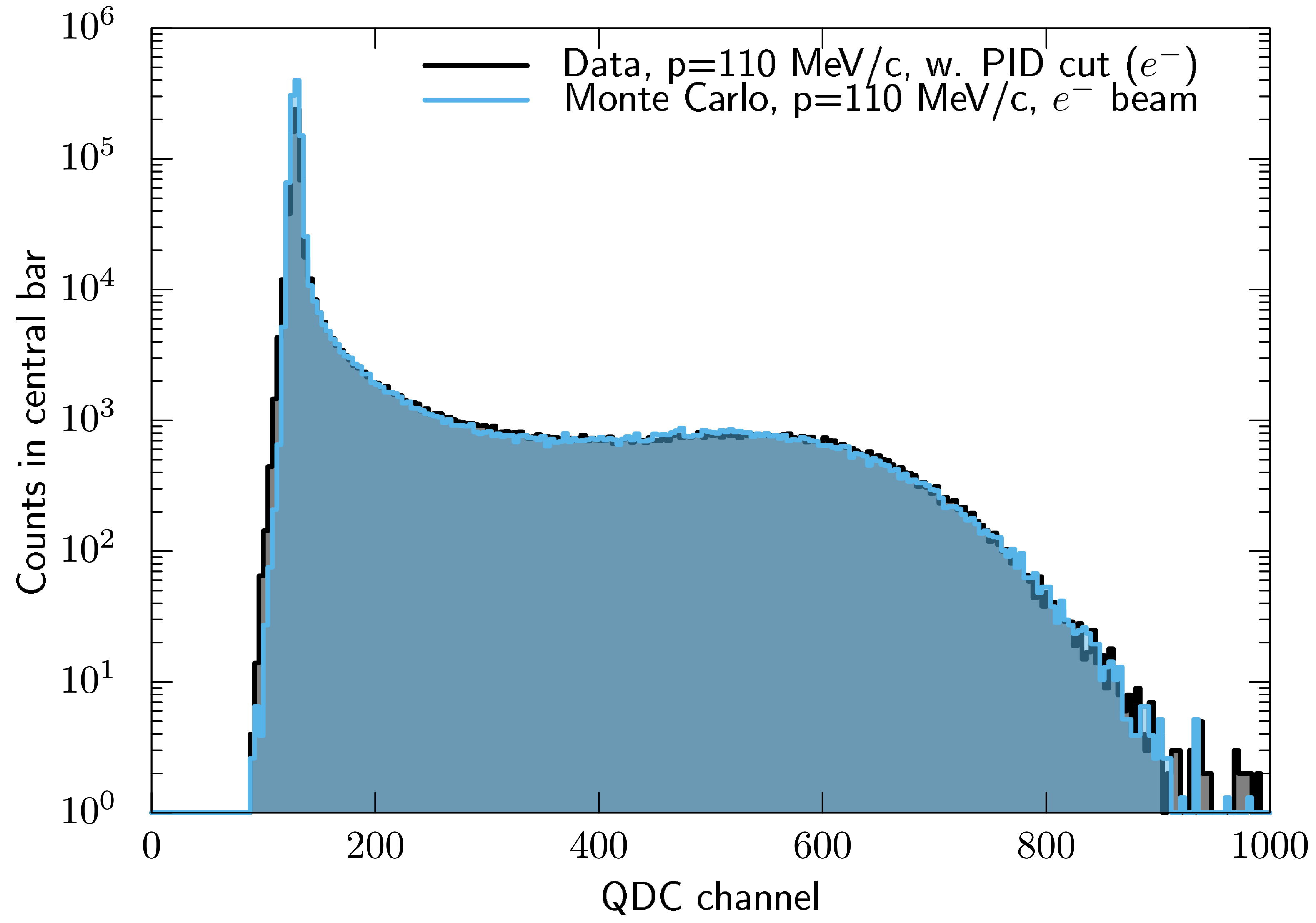

GEM digitization of simulated data

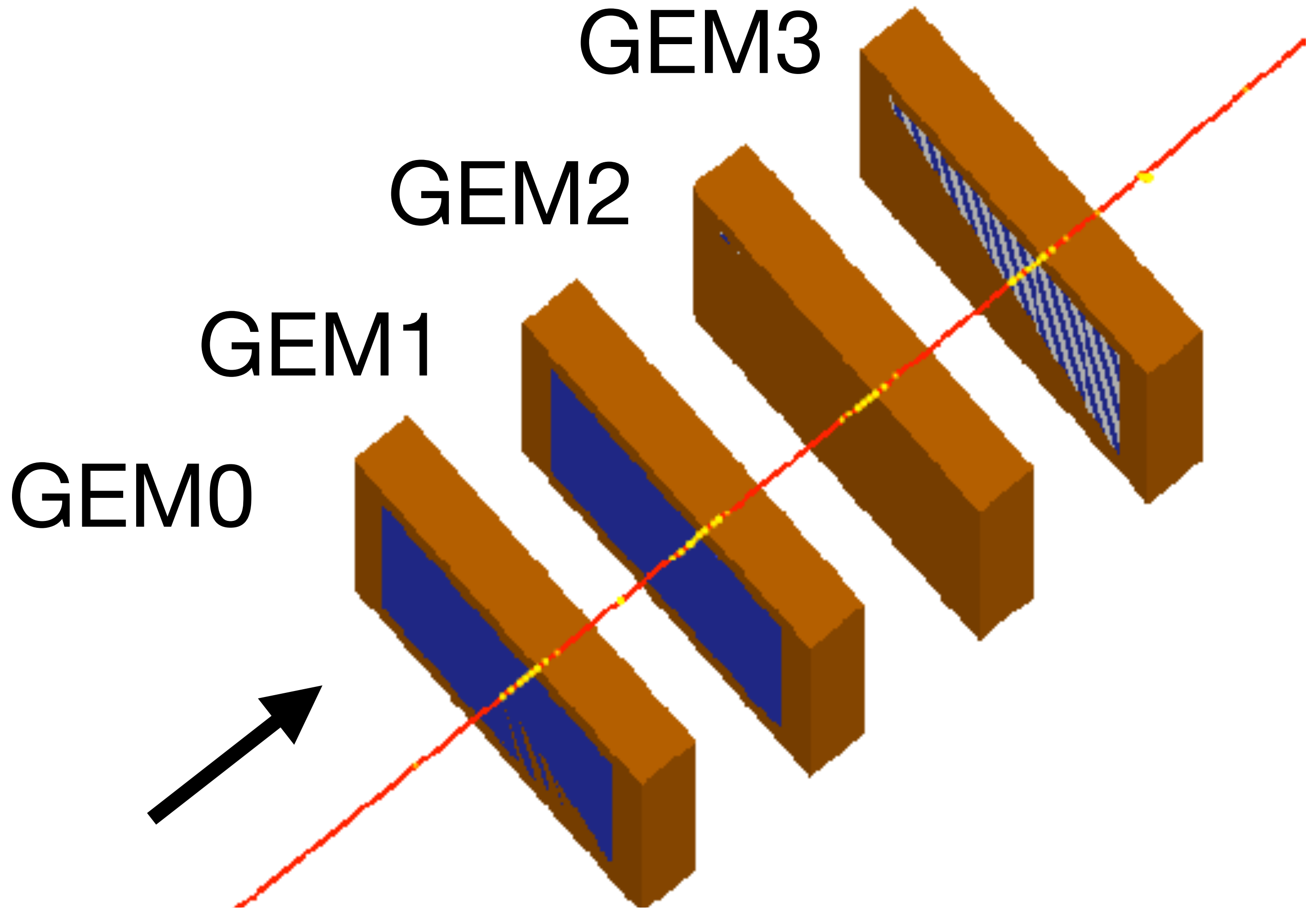

- Mapping of hit position into struck strip numbers for both axis
- Modeling of hit pattern on strips
- Suppression of dead channels
- Conversion to ADC values (including channel pedestal, and with currently fixed gain, noise)
- Per APV common mode noise

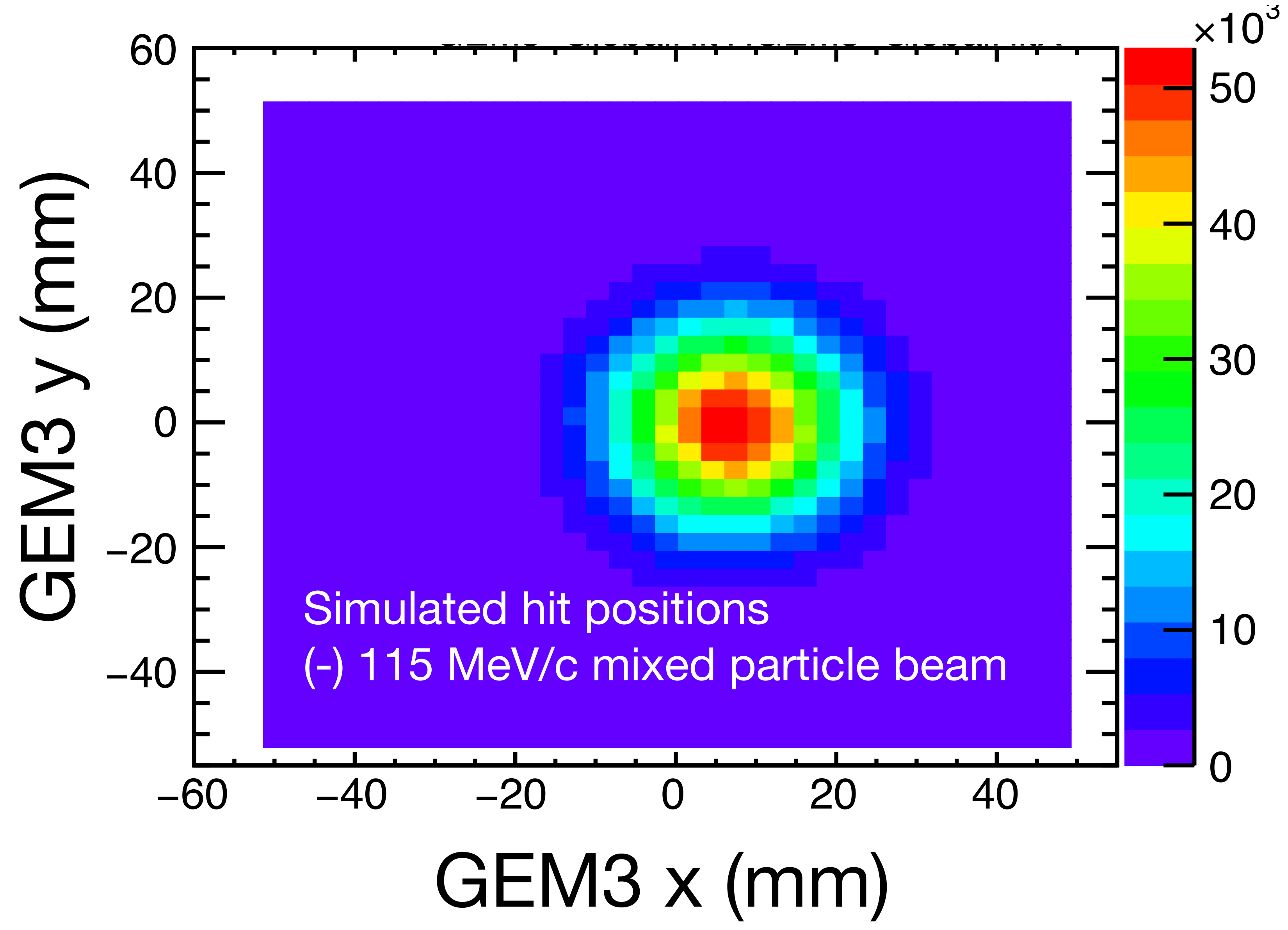

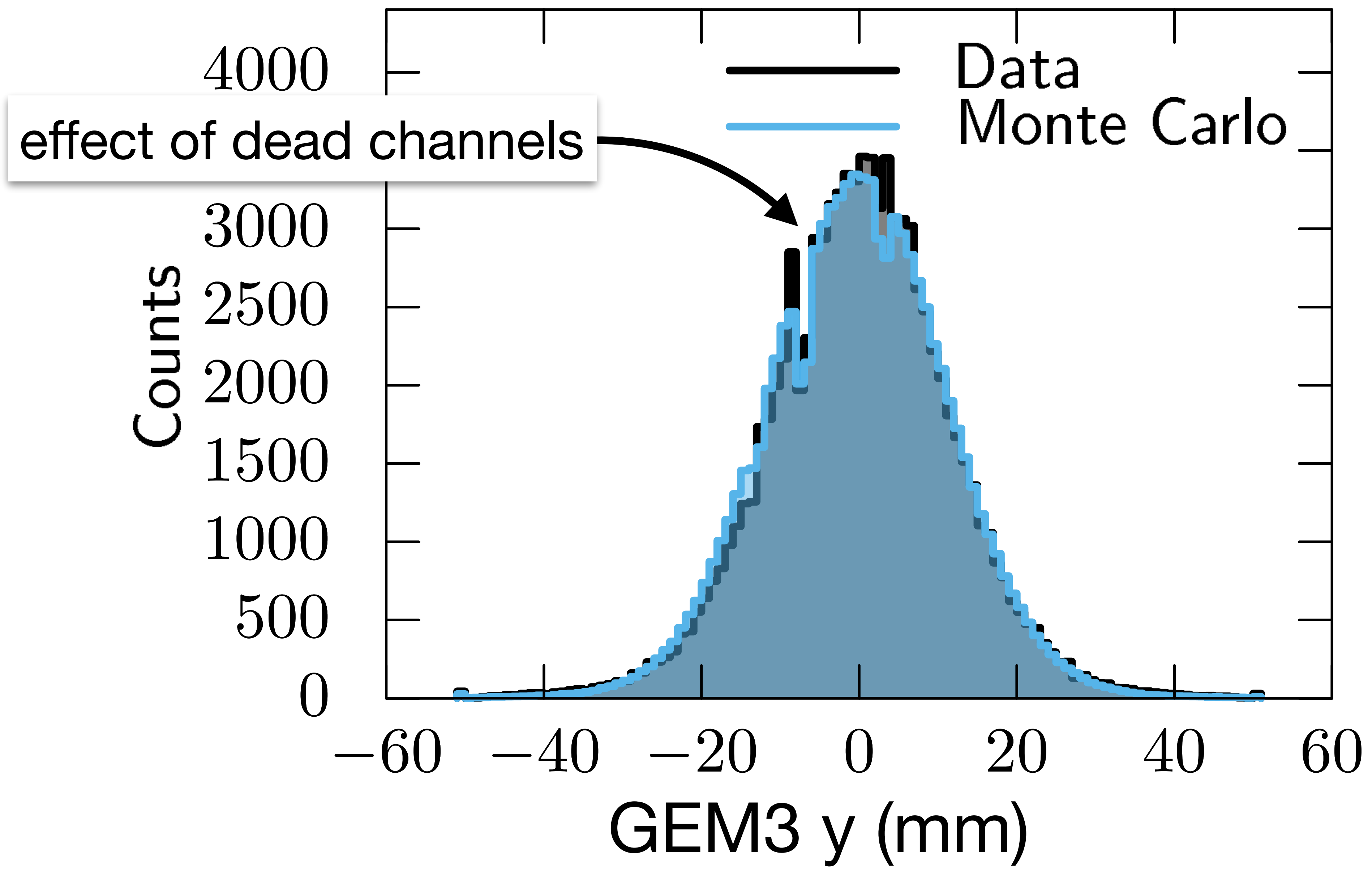

STT digitization of simulated data

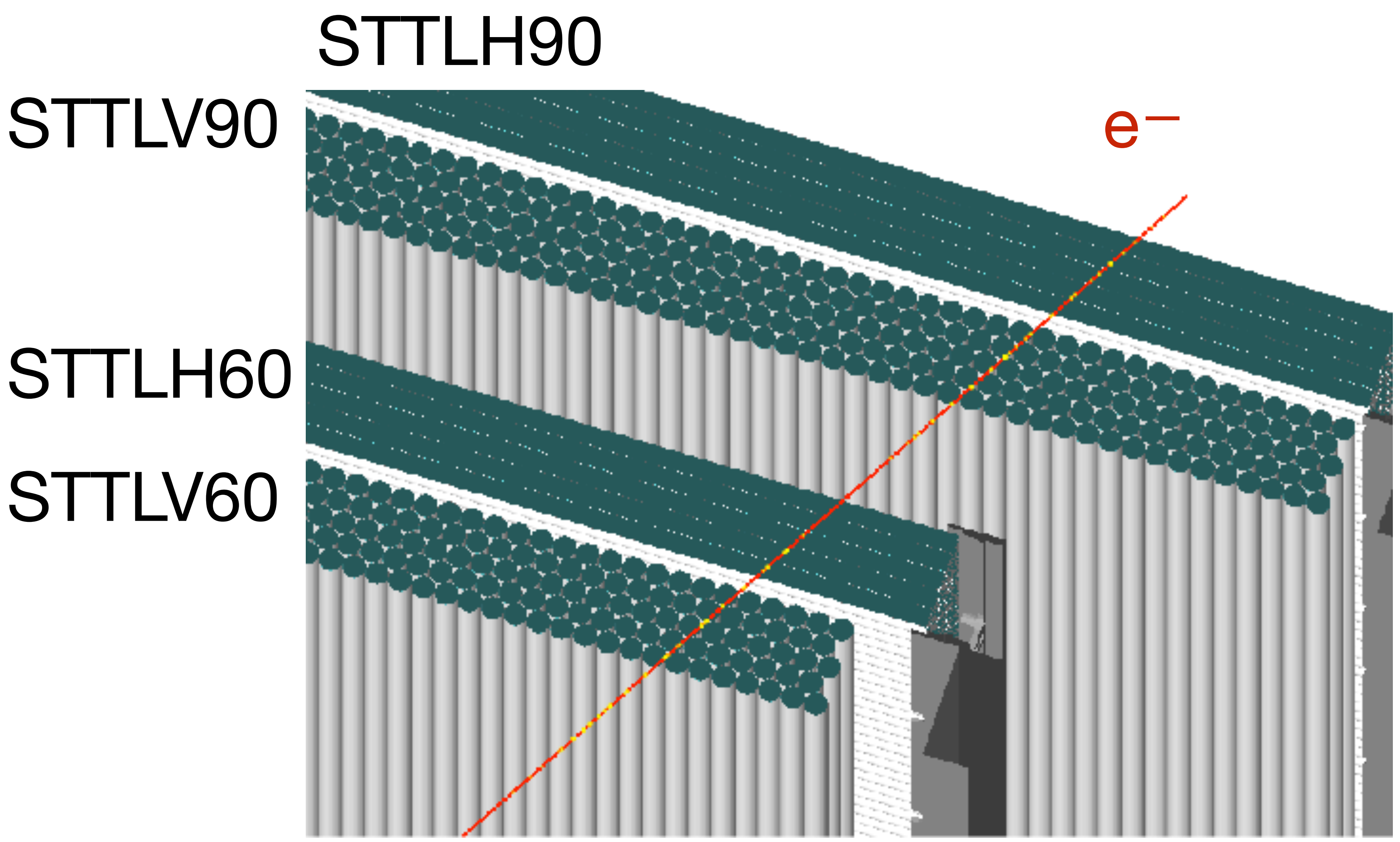

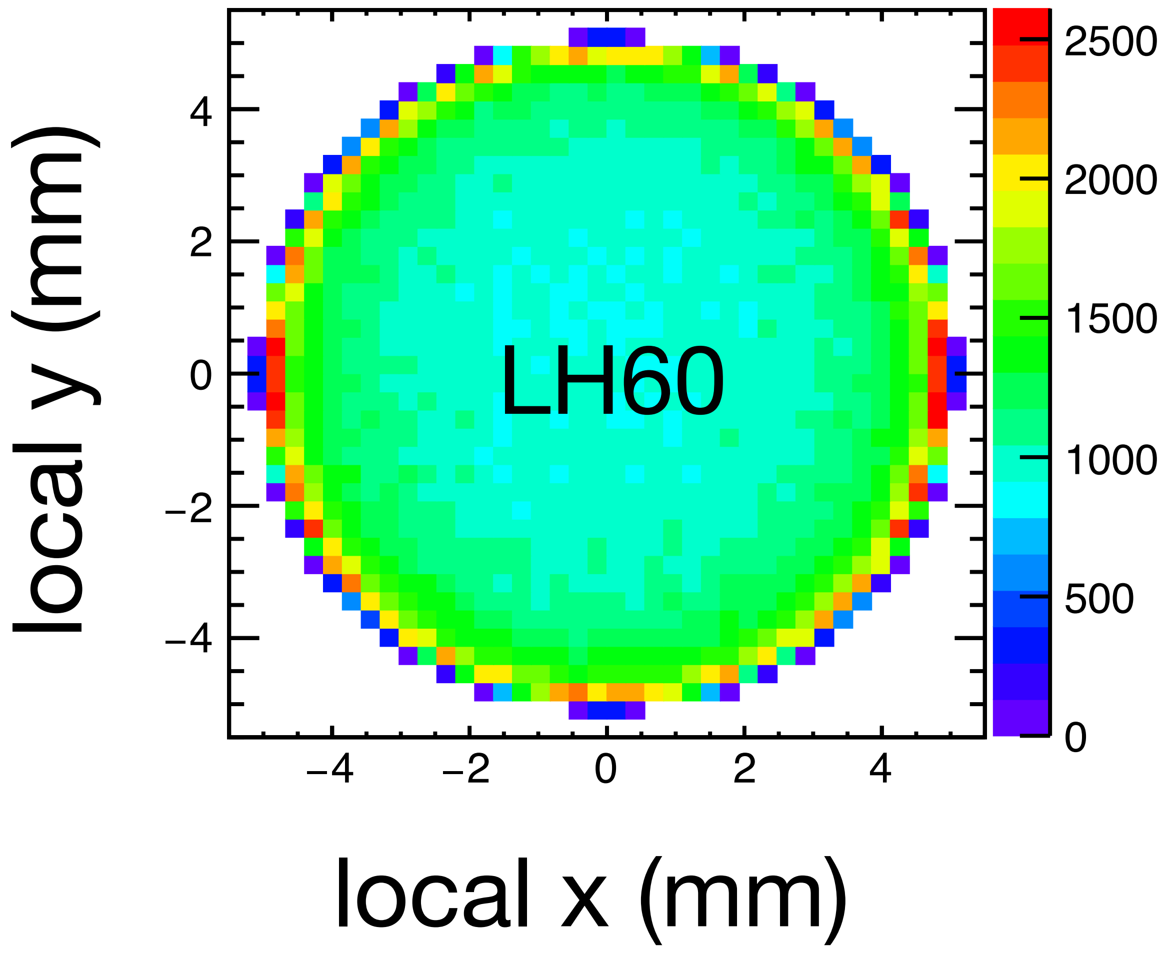

- Straws are identified by copy-ID numbers
- Local hit positions and directions are converted to drift distances and drift times that include effective resolutions
- Suppression of dead channels

Drift-time distribution

LH60 Plane 1

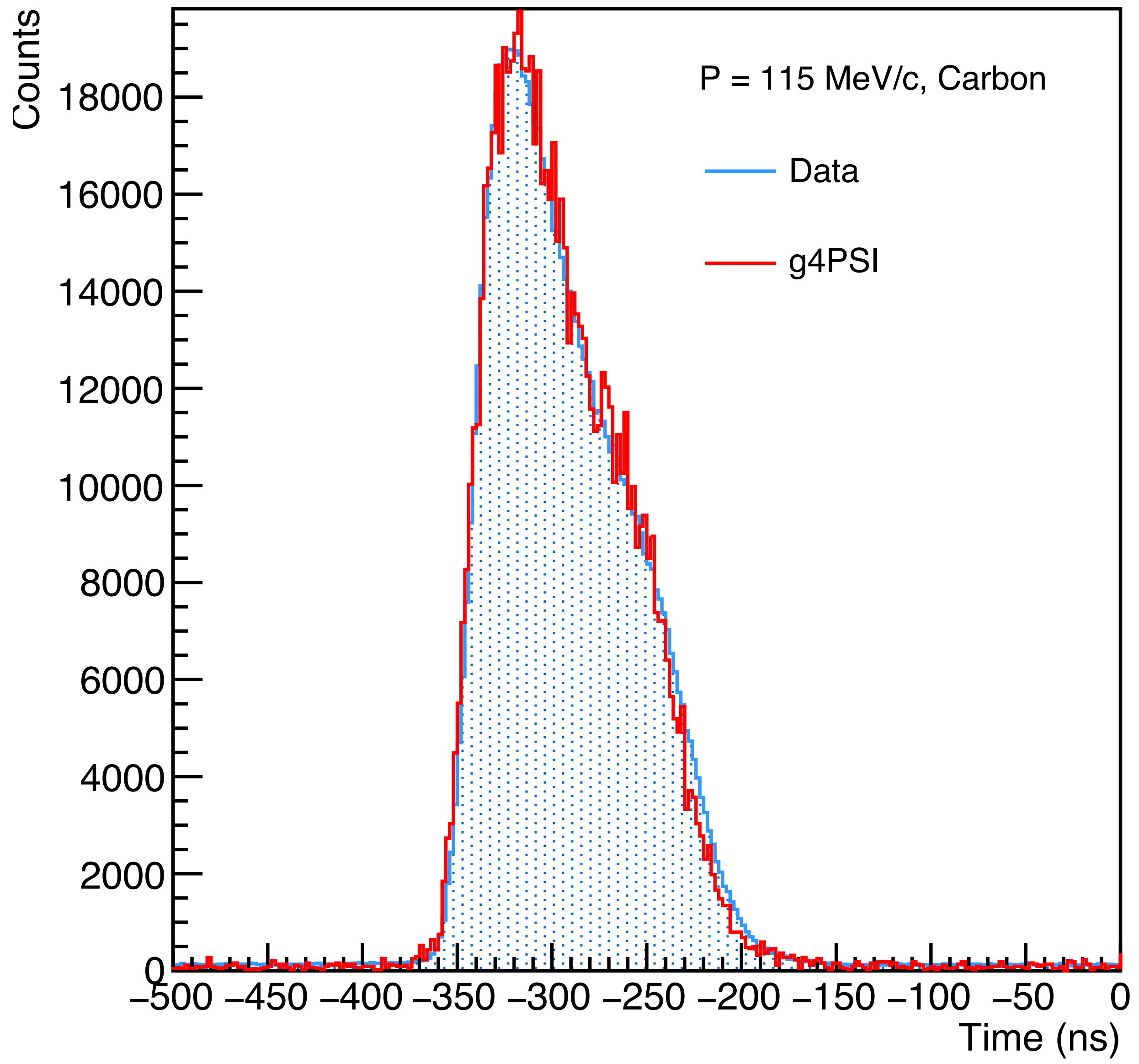

Straw distribution

LH60 Plane 1

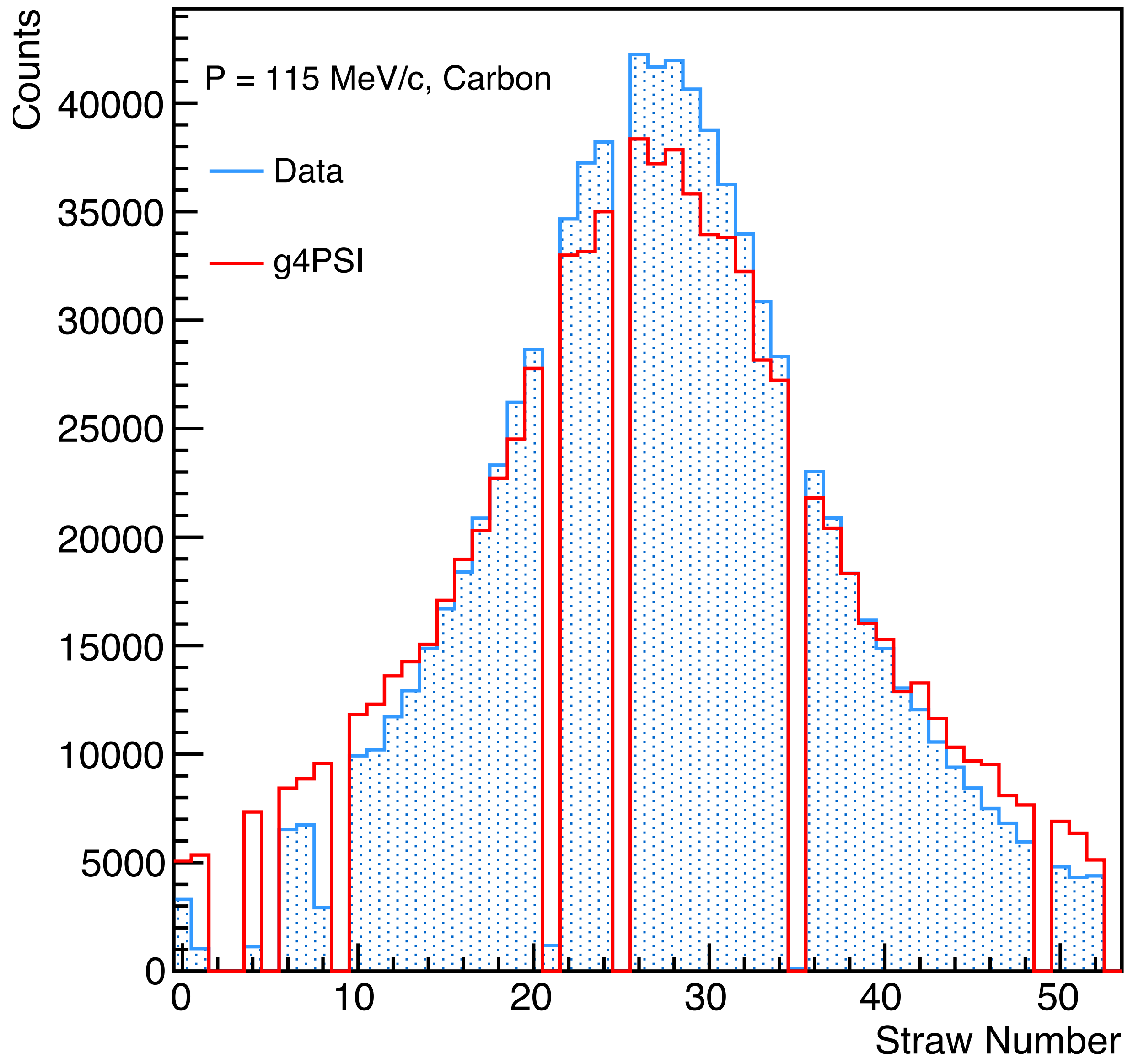

ESEPP in g4PSI - initial version

$p_0 = 161$ MeV/c
$\theta \approx 60^\circ$

Examples: $ep \to e'p\gamma$

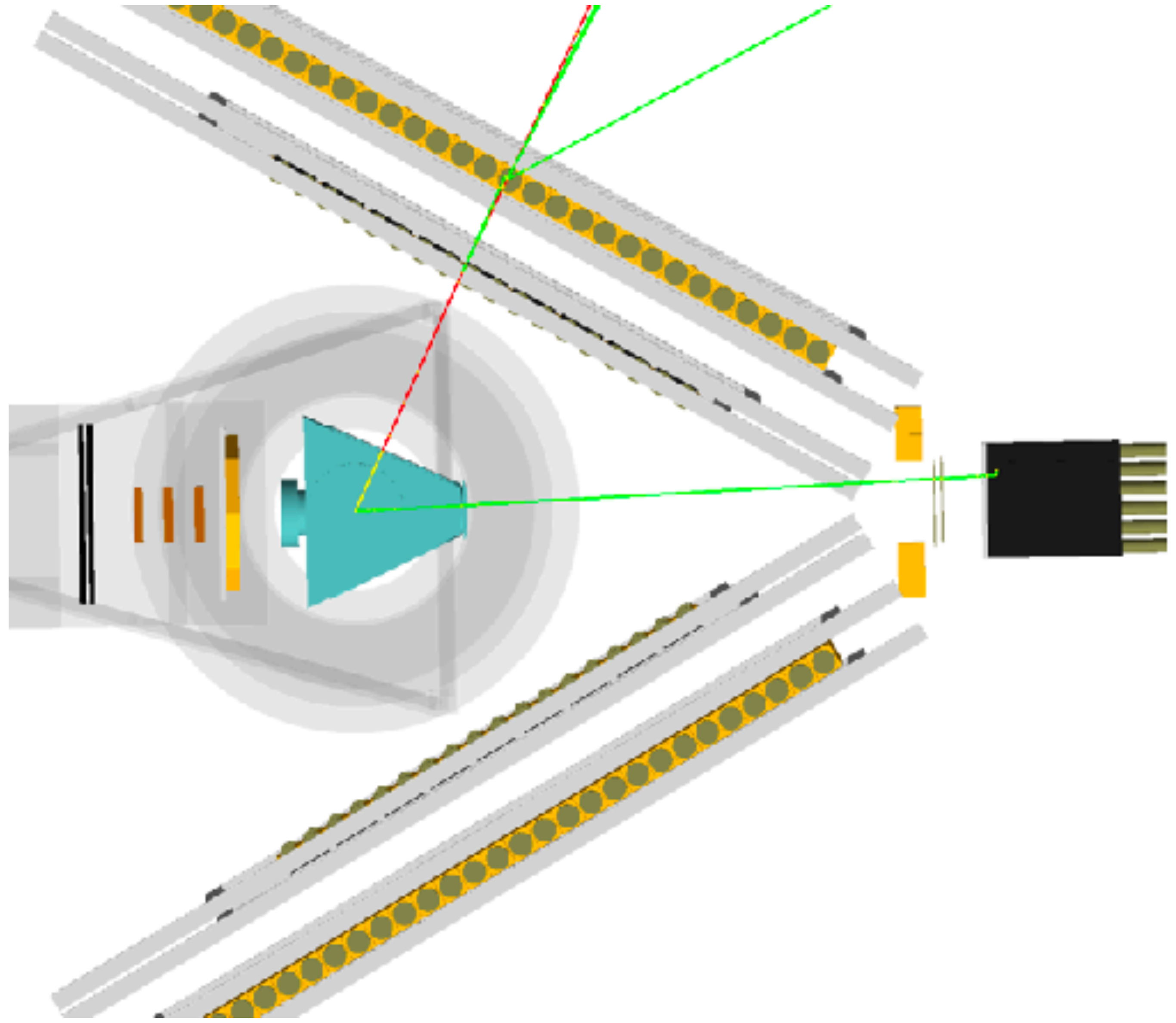

Initial-state radiation
low photon energy

$p'_e > p'_{min}$

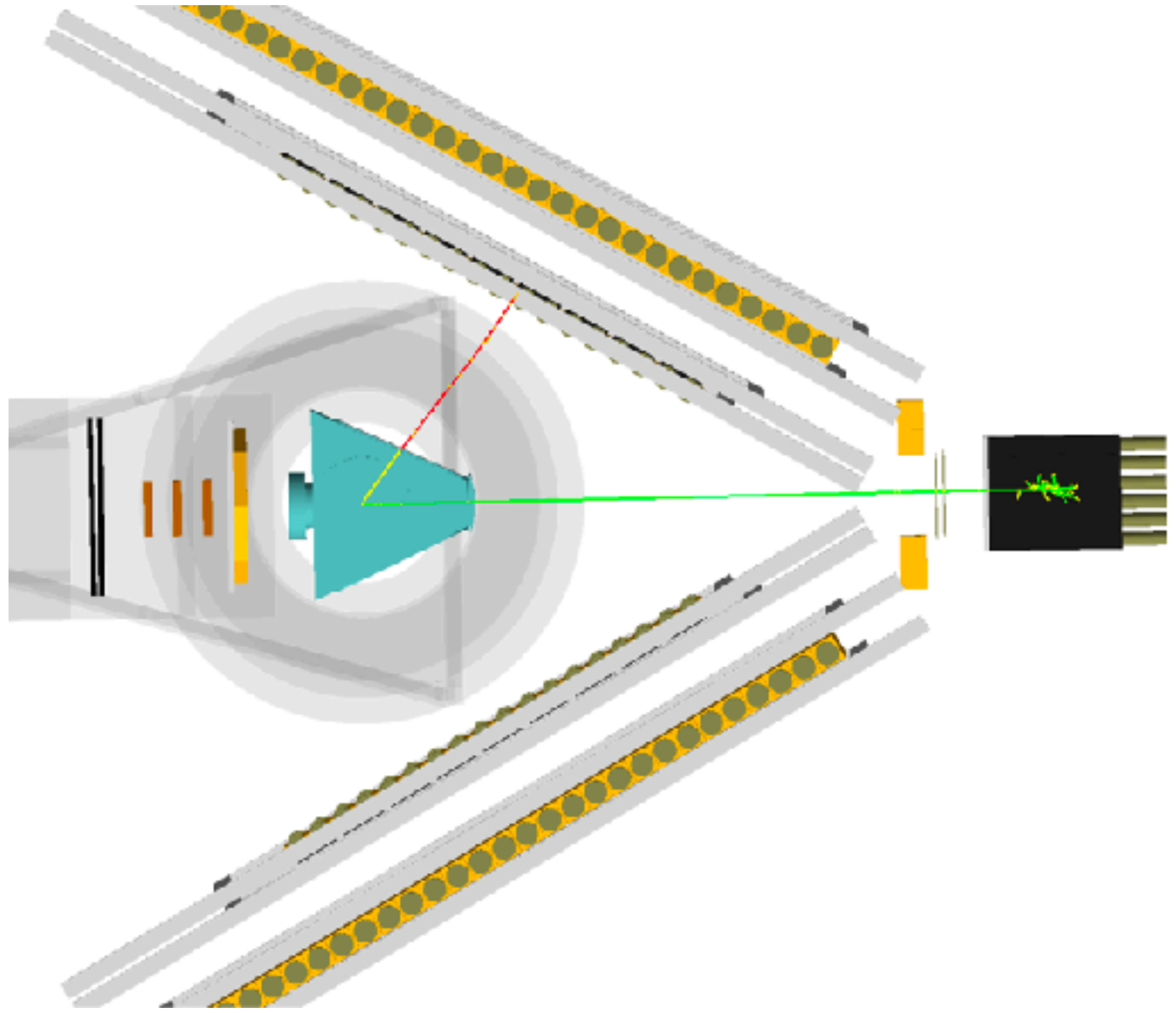

Initial-state radiation
high photon energy

$p'_e < p'_{min}$

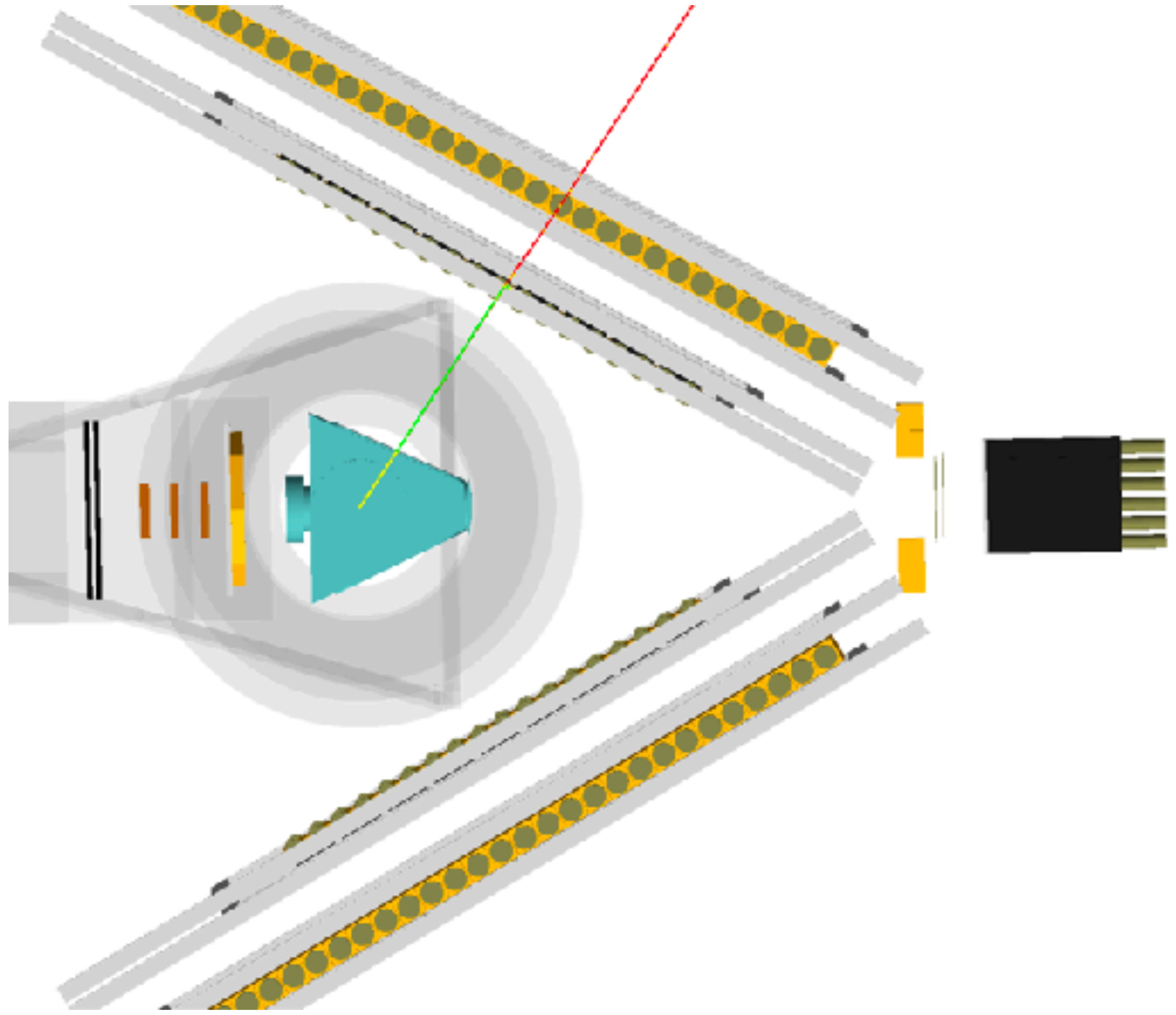

Final-state radiation

ESEPP: A.V. Gramolin et al., J. Phys. G: Nucl. Part. Phys. 41 (2014) 115001

Radiative corrections for $e^{-}p$ scattering data in MUSE kinematics

CAL veto on downstream photons reduces radiative corrections and p'_{min} dependence, reducing uncertainty.

The preliminary estimates of the total uncertainties in the radiative corrections for electrons are **0.2% - 0.5%**.

Angle-dependent uncertainty, relevant for radius extraction, ≲ **0.3%**.

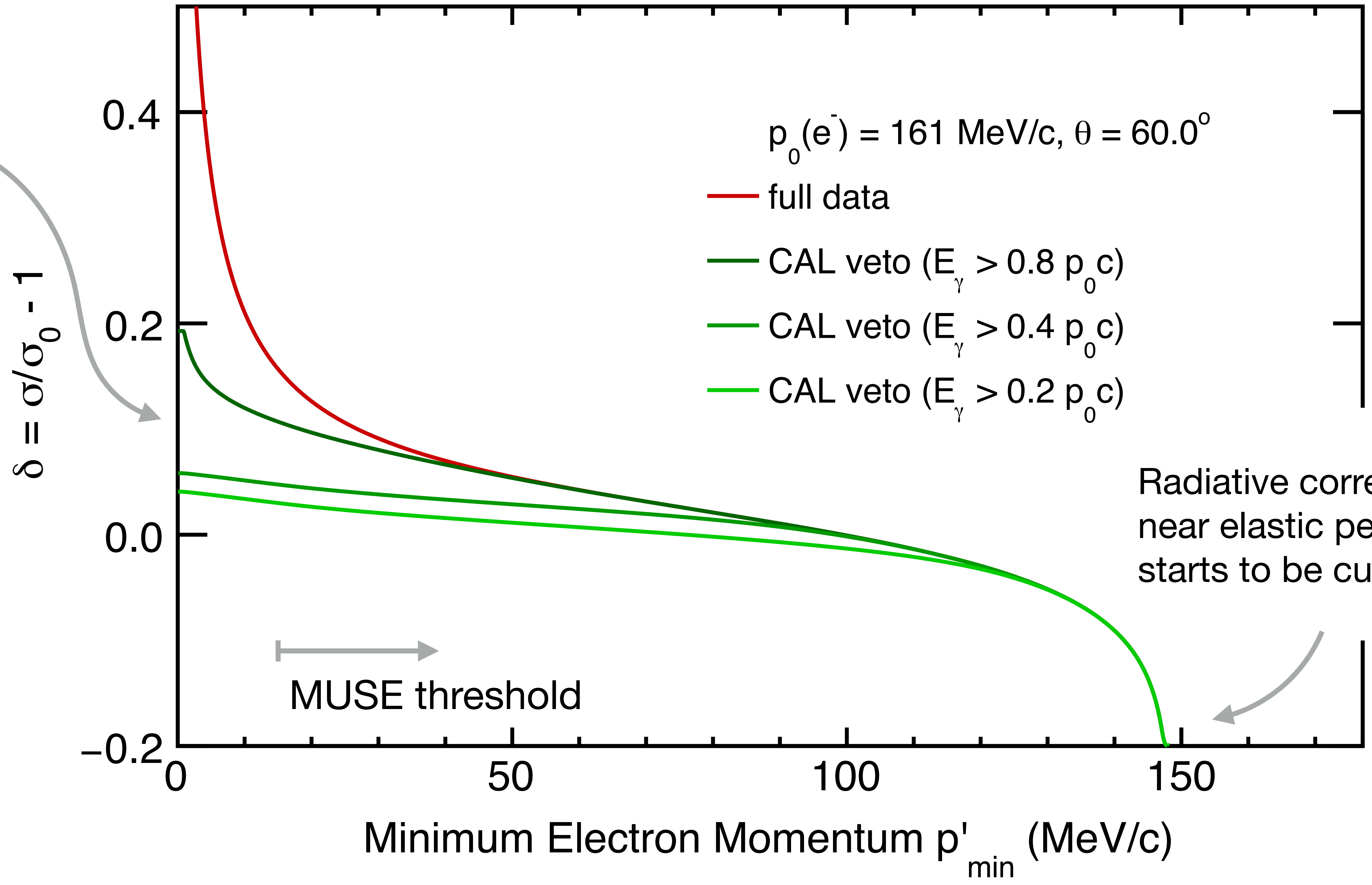

Radiative correction grows near elastic peak as it starts to be cut away.

Much more work to be done …

- Geometry
  - Include all relevant structure material (in/out scattering, background source)
  - Setup and alignment (run-time dependent)
- Running the simulation
  - Finalize model and tune of particle beams
  - Rare-event simulations
  - Include relevant physics processes (radiative processes)
- Digitization
  - Finalize the implementation of the digitization methods
  - Digitization of trigger conditions, as well as RF and trigger times
  - Tune of detector parameters (run-time dependent)
  - Slow-control data in the simulation output